The Crop Journal xxx (xxxx) xxx

Contents lists available at ScienceDirect

The Crop Journal

journal homepage: www.keaipublishing.com/en/journals/the-crop-journal/

DaMYB75 and DaMYB56 antagonistically regulate anthocyanin biosynthesis by binding to the *DaANS* promoter in *Dioscorea alata*

Xin Chen [a,b,1], Jingyu Sun [a,d,1], Nan Shan [a], Asjad Ali [c], Sha Luo [a], Shenglin Wang [a], Qianglong Zhu [a], Yao Xiao [a], Zihao Li [a], Yufan Fang [a], Jiali Lin [a], Xiaorong Chen [d,*], Qinghong Zhou [a,*], Yingjin Huang [a,d,*]

[a] *Jiangxi Province Key Laboratory of Vegetable Cultivation and Utilization, Jiangxi Agricultural University, Nanchang 330045, Jiangxi, China*
[b] *Key Laboratory of Research and Development of Natural Product from Li Folk Medicine of Hainan Province, Institute of Tropical Bioscience and Biotechnology, Chinese Academy of Tropical Agricultural Sciences, Haikou 571101, Hainan, China*
[c] *Queensland Department of Primary Industries, PO Box 1054, Mareeba, QLD 4880, Australia*
[d] *Key Laboratory of Crop Physiology, Ecology and Genetic Breeding, Ministry of Education, Jiangxi Agricultural University, Nanchang 330045, Jiangxi, China*

ARTICLE INFO

Article history:
Received 4 September 2024
Revised 8 January 2025
Accepted 24 March 2025
Available online xxxx

Keywords:
Dioscorea alata L.
Anthocyanin biosynthesis
DaMYB75
DaMYB56
DNA methylation

ABSTRACT

The yam *Dioscorea alata* L. is widely cultivated globally. Purple-fleshed varieties of this important crop have enhanced market value due to their high anthocyanin contents, but how anthocyanin biosynthesis in *D. alata* tubers is regulated remains poorly understood. In this study, we identified and functionally validated key transcription factors that regulate anthocyanin biosynthesis based on a comparative transcriptome and metabolome analysis of three *D. alata* cultivars with different colored tubers (dark purple, light purple, and white). The anthocyanin glycoside cyanidin-3-*O*-(2′′-*O*-glucosyl) glucoside was abundant during early tuber development, and we determined that its accumulation is regulated in opposite manners by two R2R3-MYB transcription factors: DaMYB75 and DaMYB56. Yeast two-hybrid and bimolecular fluorescence complementation assays in *Nicotiana benthamiana* and co-expression assays in *D. alata* demonstrated that DaMYB75 promotes anthocyanin biosynthesis by specifically activating the promoter of the late anthocyanin biosynthesis gene *DaANS* and enhancing its expression through an interaction with DabHLH72. By contrast, DaMYB56 is a negative regulator of anthocyanin biosynthesis that binds to the *DaANS* promoter together with DabHLH72. Furthermore, the methylation levels of the *DaMYB75* promoter were significantly lower in purple tubers than in white tubers. These findings shed light on the regulation of anthocyanin biosynthesis by MYBs and provide the basis for genetically improving anthocyanin content in *D. alata*.

1. Introduction

Anthocyanins, a class of natural water-soluble pigments, are secondary metabolites derived from the flavonoid branch of the phenylpropanoid pathway. These pigments are responsible for tissue color in various plant species, including the distinctive purple tubers of most varieties of purple yam (*Dioscorea alata*) [1–3]. Anthocyanins play essential roles in multiple aspects of plant biology, acting as pigments to attract pollinators and as antioxidants to protect plants from abiotic stress [4,5]. Notably, anthocyanins promote human health due to their high antioxidant activity, which helps prevent chronic diseases and protects the body from damage caused by free radicals [6–9]. Therefore, anthocyanins are increasingly being used in the food and pharmaceutical industries [10,11].

The anthocyanin biosynthetic pathway is a downstream branch of the flavonoid biosynthetic pathway, which is relatively well conserved in land plants. Flavonoid biosynthesis primarily involves two groups of structural genes encoding enzymes: early biosynthetic genes (EBGs), which include *Chalcone synthase* (*CHS*), *Chalcone isomerase* (*CHI*), *Flavanone 3-hydroxylase* (*F3H*), *Flavanone 3-hydroxylase* (*F3′H*), and *Flavonoid 3′,5′-hydroxylase* (*F3′5′H*); and late biosynthetic genes (LBGs), which include *Dihydroflavonol 4-reductase* (*DFR*), *Anthocyanidin synthase* (*ANS*), *Anthocyanidin reductase* (*ANR*), *Leucoanthocyanidin reductase* (*LAR*), and *UDP-glucose: flavonoid 3-O-glycosyl transferase* (*UFGT*). The enzymes encoded by EBGs produce the biosynthetic precursors used by all branches

* Corresponding authors.
E-mail addresses: ccxxrr80@jxau.edu.cn (X. Chen), qinghongzhou@jxau.edu.cn (Q. Zhou), huangyying@jxau.edu.cn (Y. Huang).
[1] The authors contributed equally to this study.

https://doi.org/10.1016/j.cj.2025.03.009

of the flavonoid pathway, whereas those encoded by LBGs are specific to anthocyanin and proanthocyanidin biosynthesis [5,12,13].

The expression of EBGs and LBGs is typically regulated by specific R2R3-MYB and basic helix-loop-helix (bHLH) family members, as well as other transcription factors [14–16]. Among these, R2R3-MYBs from the S6 subgroup are crucial positive regulators of anthocyanin biosynthesis [17]; bHLHs associated with flavonoid biosynthesis belong to subgroup IIIf, which can form MYB-bHLH complexes with MYBs [18,19]. Great progress has been made in investigating the transcriptional regulation of anthocyanin metabolism shaping the color of flowers and fruits from horticultural crops. For example, the R2R3-MYB transcription factors DEEP PURPLE (DPL) and PURPLE HAZE (PHZ) interact with the basic helix-loop-helix (bHLH) transcription factor ANTHOCYANIN1 (AN1) and the WD-repeat protein AN11 to regulate anthocyanin biosynthesis in petunia (*Petunia hybrida*), including anthocyanin production in vegetative tissues, and contribute to floral pigmentation [20]. In apple (*Malus domestica*), MdMYB3, MdMYB9, MdMYB11, MdbHLH3, MdWRKY72, LONG HYPOCOTYL 5 (MdHY5), and other transcription factors enhance anthocyanin biosynthesis by directly or indirectly activating the expression of related biosynthetic genes [21–23]. There has been increasing interest in the mechanisms that regulate anthocyanin production in the underground structures of root crops, such as the functions of the transcription factors DcMYB113 and DcbHLH3 in anthocyanin biosynthesis in carrots (*Daucus carota*) [24,25]. Similarly, the bHLH transcription factor AcB2 improves the ability of AcMYB1 to increase anthocyanin production in onions (*Allium cepa*) [19].

Some MYB transcription factors function as repressors of anthocyanin biosynthesis [26]. For example, AtMYB3, AtMYB4, AtMYB7, and AtMYB32 from the S4 subgroup function as transcriptional inhibitors of lignin biosynthesis, drought-stress responses, and anthocyanin biosynthesis in Arabidopsis (*Arabidopsis thaliana*) [27–29]. In addition, genes homologous to members of this subgroup inhibit anthocyanin biosynthesis in plant species such as peach (*Prunus persica*), grapevine (*Vitis vinifera*), and poplar (*Populus tremula*) [30–32]. Similarly, in red-fleshed apple callus, MdMYB16 suppress the expression of *MdUFGT* and *MdANS* as well as anthocyanin biosynthesis [33]; MaMYB4 negatively regulates the biosynthesis of anthocyanin in bananas (*Musa acuminata*) [34].

DNA methylation also influences anthocyanin biosynthesis in horticultural plant species. For instance, in radish (*Raphanus sativus*), alterations in the DNA methylation levels of the *RsMYB1* promoter result in white-fleshed roots [35]. Similarly, DNA methylation levels along the promoters of structural genes are potentially linked to the development of petal blotch on Xibei tree peony (*Paeonia rockii*) [36]. Furthermore, anthocyanin biosynthesis is regulated via DNA methylation in fruits such as apple, pear (*Pyrus pyrifolia*), and orange (*Citrus sinensis*) [37–39].

Purple yam (*Dioscorea alata* L.), a crop from the genus *Dioscorea* in the family Dioscoreaceae, is the yam species most extensively cultivated around the globe [40,41]. Transcriptome analysis revealed the significant upregulation of the anthocyanin biosynthesis-related genes *CHS*, *F3H*, *F3H*, *DFR*, *ANS*, and *UF3GT* in a *D. alata* cultivar with purple tuber flesh compared to a *D. alata* cultivar with white tuber flesh [42]. In addition, the expression levels of *Phenylalanine ammonia-lyase* (*PAL*), *F3H*, *ANS*, and *UFGT*, encoding enzymes related to anthocyanin biosynthesis, exhibited some correlation with anthocyanin accumulation rates in various organs of *D. alata* [43]. However, to date, no transcription factors have been characterized as regulators of anthocyanin biosynthesis in *D. alata* tubers. In this study, we performed metabolome and transcriptome analyses of *D. alata* cultivars with contrasting flesh colors, together with phylogenetic analysis, to identify key transcription factors that regulate anthocyanin biosynthesis. We validated the functions of these candidates in regulating anthocyanin biosynthesis in a purple *D. alata* cultivar, establishing a molecular basis for the anthocyanin biosynthesis pathway in *D. alata*.

2. Materials and methods

2.1. Plant materials

Three *D. alata* cultivars were used in this study: Ganzishi 2 with pure purple tubers (pp), Ganziyun 1 with faint purple tubers (fp), and Ganbaiyu 1 with pure white tubers (pw) (Fig. 1A; Table S1). All plants were planted in a yam germplasm resource garden in Jiangxi Agricultural University (28.77°N, 115.84°E, Nanchang, Jiangxi, China) on April 17, 2022. Standard field practices, including appropriate fertilization, irrigation, and management of diseases and pests, were employed. Tubers in good condition with the same growth status were randomly harvested at 120, 135, 150, 165, and 180 d after planting (DAP). The tubers were peeled and cut into small pieces before being used for metabolome analysis, transcriptome sequencing, and anthocyanin measurements. The tuber epidermis, tuber flesh, roots, stems, and young leaves were collected at different DAP for RT-qPCR analysis and anthocyanin measurements. All samples were flash-frozen and stored at −80 °C. For all samples, three biological replicates were used, with each biological replicate containing five plants.

Long-day climate chambers (16-h light/8-h dark, 25 °C/23 °C [day/night]) were used to cultivate tobacco (*Nicotiana tabacum* cultivar K326), *N. benthamiana*, and *D. alata* cultivars Ganbaiyu 1 (pw) and Ganzishi 2 (pp).

2.2. Extraction and quantification of anthocyanins

Anthocyanins were extracted from the samples as described by Vatai et al. [44] with some modifications. In brief, 1 g chopped, homogenized fresh tuber tissue was extracted by incubating in extraction solution (acetone: distilled water: formic acid = 80:19.8:0.2, v/v/v) and shaking for 30 min at 4 °C. Chloroform was added to leaf samples to remove chlorophyll. The optical density (OD) of the supernatants was measured at 520 nm and 700 nm.

2.3. Metabolome analysis and transcriptome sequencing

Identification and extraction of flavonoids were conducted by Metware Biotechnology Co., Ltd. (Wuhan, Hubei, China). Flavonoids were extracted from samples collected at two stages: 135 DAP (pp2, fp2, and pw2) and 180 DAP (pp5, fp5, and pw5), with three biological replicates for each of the three cultivars. Analysis of the 18 resulting samples (three cultivars × two sampling times × three biological replicates) was conducted on a UPLC-ESI-MS/MS system (UPLC, SHIMADZU Nexera X2; MS, Applied Biosystems 4500 Q TRAP). Utilizing the range method, the metabolite content data were normalized with R software (https://www.r-project.org/). The criteria $|\log_2(\text{fold change})| \geq 1$ and variable importance in projection (VIP) ≥ 1 were used to distinguish between groups with differential metabolite accumulation. Kyoto Encyclopedia of Genes and Genomes (KEGG) pathway enrichment analysis was performed using the differentially abundant metabolites.

Metware Biotechnology Co., Ltd. conducted the sequencing of RNA-seq libraries from pp2, fp2, pw2, pp5, fp5, and pw5 tuber samples. An NEBNext Ultra RNA Library Prep Kit for Illumina

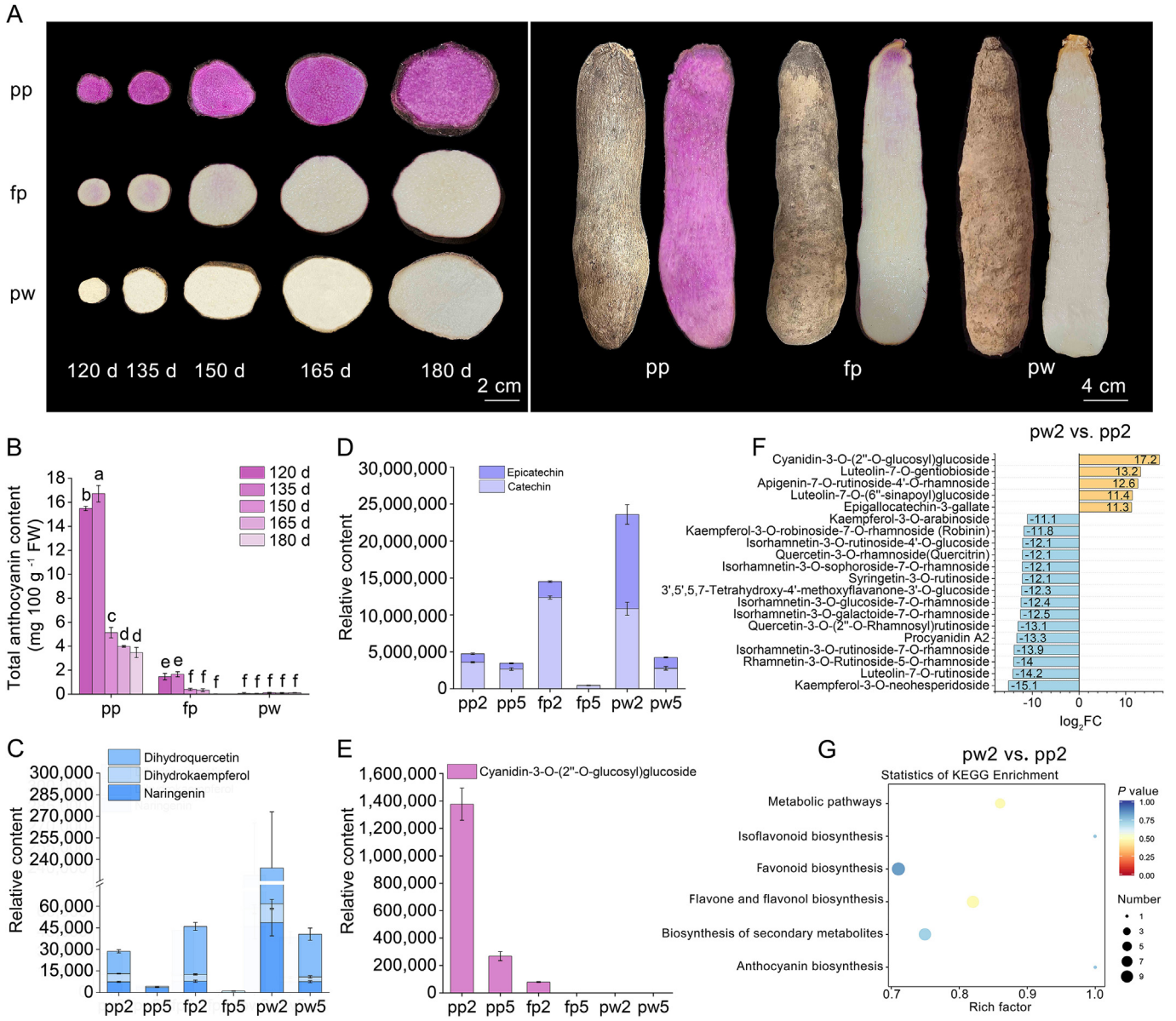

Fig. 1. Metabolome analysis of *D. alata* cultivars with purple or white tubers. (A) Representative photographs of tubers from three *D. alata* cultivars, pp (pure purple tuber), fp (faint purple tuber) and pw (pure white tuber), at different developmental stages. Left, cross-sections of the middle tuber; right, whole tubers and longitudinal sections at 180 days after planting (180 d). (B) Total anthocyanin content in pp, fp, and pw tuber flesh at the indicated developmental stages. FW, fresh weight. Values are means ± standard error from three biological replicates. Different lowercase letters indicate significant differences, as determined by one-way analysis of variance (ANOVA), with $P < 0.05$. (C–E) Relative dihydroquercetin, dihydrokaempferol, naringenin, epicatechin, catechin, and cyanidin-3-*O*-(2′′-*O*-glucosyl) glucoside contents in tubers of the pp, fp, and pw cultivars at 135 d (indicated by 2) and 180 d (indicated by 5) after planting. (F) Top 20 differentially abundant metabolites between pw2 and pp2. Metabolites that are more abundant in pp2 are shown in red, whereas less abundant metabolites are shown in green. (G) KEGG pathway enrichment analysis of the differentially abundant metabolites between pw2 and pp2. Circle size reflects the number of distinct metabolites, and the circle color reflects the *P*-value.

(NEB, Ipswich, MA, USA) was employed to construct the cDNA libraries following the manufacturer's instructions. The sequencing libraries were sequenced on the Illumina HiSeq NovaSeq 6000 platform (Illumina, Inc., San Diego, CA, USA). Overall, 126.67 Gb of clean data were produced, averaging 7.04 Gb per sample. The percentage of bases that scored ≥ Q30 was 92.2% (Table S2). Differentially expressed genes (DEGs) were defined as those having a $|\log_2(\text{fold change})| \geq 1$ and a false discovery rate (FDR) < 0.05. The KEGG Ortholog database was used for pathways enrichment analysis of the DEGs. Weighted gene co-expression network analysis using the transcriptome and metabolome data was performed using WGCNA v1.69.

2.4. Identification of DaR2R3-MYB and DabHLH family members and phylogenetic analysis

The whole genome sequence of *D. alata* was obtained from the yam genome database (https://yambase.org/) [45], and the longest transcript of each gene was extracted for analysis. The amino acid sequences of Arabidopsis R2R3-MYB and bHLH transcription factors were downloaded from The Arabidopsis Information Resource (https://www.arabidopsis.org/) and used as queries against the *D. alata* genome by BLASTP. The phylogenetic trees were reconstructed with MEGA (v.7) using the neighbor-joining method and 1000 bootstrap repetitions [46].

2.5. Total RNA and DNA extraction, RT-qPCR analysis, and isolation of candidate genes and promoter sequences

Total RNA extraction (0416-50gk, Huayueyang, Beijing, China), total DNA extraction (9768, Takara, Shiga, Japan), and first-strand cDNA synthesis (11139ES60, Yeasen, Shanghai, China) were performed as per the directions provided by each manufacturer. Subsequently, SYBR Green Master Mix (11184ES08, Yeasen, Shanghai, China) was used for qPCR analysis in 20 μL reactions, with three biological replicates and three technical replicates per biological replicate. The sequences of the candidate genes and their promoters were amplified by PCR using Plus PCR Master Mix (10154ES01, Yeasen, Shanghai, China). The prediction of *cis*-elements in the promoter sequences was performed by uploading the sequences to the PlantCARE online tool (https://bioinformatics.psb.ugent.be/webtools/plantcare/html/). Table S3 lists the primers used for genomic PCR and RT-qPCR.

2.6. Bisulfite sequencing PCR (BSP) assay

The BSP assay was performed as previously described [35]. High-quality genomic DNA from the tuber flesh of the pp and pw cultivars was treated with an EZ DNA Methylation-Gold Kit (D5006, Tianmo, Beijing China) following the manufacturer's guidelines. The *DaMYB75* (−1623 bp to −1 bp, with +1 representing the A of the translation initiation codon) promoter was divided into four fragments (−1561 bp to −1300 bp, −1214 bp to −988 bp, −891 bp to −663 bp, and −385 bp to −123 bp) containing all the CG sites. The bisulfite-treated genomic DNA served as a template for the amplification of these fragments using relevant degenerate primers (Table S3). After purifying the PCR products and ligating them into the pMD18-T vector for Sanger sequencing, Kismeth (https://katahdin.girihlet.com/kismeth/revpage.pl) online software was used to analyze 10 independent clones per segment.

2.7. Transient expression assays in N. benthamiana and D. alata, stable transformation of N. tabacum

The full-length coding sequences of *DaMYB75*, *DaMYB56*, *DabHLH32*, and *DabHLH72* were individually cloned into the pBI121 vector. The resulting plasmids were individually introduced into Agrobacterium (*Agrobacterium tumefaciens*) strain GV3101. Young and fully expanded leaves of *D. alata* plants were infiltrated with Agrobacterium cell suspensions harboring one target plasmid or the empty vector in infiltration buffer (10 mmol L^{-1} MES, 10 mmol L^{-1} $MgCl_2$, 200 μmol L^{-1} acetosyringone, pH 5.5–5.7) to a final OD_{600} = 0.8. The infiltration of *N. benthamiana* leaves was performed as described by Sparkes et al. [47]. Agrobacterium cell suspensions each carrying a different plasmid were mixed in equal volume following resuspension in infiltration buffer and co-infiltrated into leaves. Samples were collected from the infiltration sites following 1–2 weeks of normal cultivation to quantify anthocyanin contents and analyze gene expression.

A specific 300-bp fragment of the *DaMYB75* coding sequence was cloned into the pTRV2 vector and introduced into Agrobacterium strain GV3101. Positive Agrobacterium colonies, each containing the resulting pTRV2:*DaMYB75* vector, the auxiliary pTRV1 vector, and the viral silencing suppressor P19, were resuspended in infiltration buffer (10 mmol L^{-1} MES, 10 mmol L^{-1} $MgCl_2$, 200 μmol L^{-1} acetosyringone, pH 5.5–5.7) and mixed at a 1:1:1 (v/v/v) ratio. As a control, Agrobacterium colonies each harboring the empty pTRV2 vector, the auxiliary pTRV1 vector, or P19 were resuspended in infiltration buffer, mixed at a 1:1:1 (v/v/v) ratio, and infiltrated into small tubers of pp plants cultivated *in vitro* [48]. After infiltration, the tubers were placed in an incubator at 25 °C in the dark. After one week, the flesh near the infiltration site was harvested for phenotypic analysis and RT-qPCR assays. The primers used in this study are listed in Table S3.

Stable transformation of tobacco (*N. tabacum* cultivar K326) was performed as described by Pattanaik et al. [49], using the same vectors as for subcellular localization. The leaves and flowers of transgenic T_3 and wild-type plants were used to analyze anthocyanin contents and gene expression levels. The primers used for cloning are listed in Table S3.

2.8. Subcellular localization of DaMYB75, DaMYB56, DabHLH32, and DabHLH72

Constructs encoding green fluorescent protein (GFP) fusions to each candidate protein were generated by individually cloning the full-length coding sequences of each transcription factor gene, without the stop codon, into the pSuper1300 vector. The plasmids were introduced into Agrobacterium strain GV3101 competent cells for transient expression in *N. benthamiana* leaves. Following 2 d of cultivation at 25 °C under a 16 h/8 h light/dark cycle, the infiltrated leaf sections or peeled epidermis were excised. A drop of DAPI staining solution (10 μg mL^{-1}) was applied, and a coverslip was placed over the sample. The samples were incubated in the dark for either 20 min or 3–5 min. GFP fluorescence was observed under a FV3000 laser-scanning confocal microscope (Olympus, Tokyo, Japan); fluorescence at 488 nm (green/GFP) and 405 nm (blue/DAPI) was observed [50]. The primers used to generate the constructs for subcellular localization are listed in Table S3.

2.9. Yeast two-hybrid (Y2H) assay

The full-length coding sequences of *DaMYB75* and *DaMYB56* were individually cloned into the pGADT7 vector, and the full-length coding sequences of *DabHLH32* and *DabHLH72* were individually cloned into the pGBKT7 vector. The Y2H assay was performed as previously reported methods [51]. During growth on selective medium, 3-AT and X-α-gal were added as an inhibitor and chromogenic substrate, respectively. The primers used for cloning the Y2H plasmids are listed in Table S3.

2.10. Bimolecular fluorescence complementation (BiFC) assay

The full-length coding sequences without the stop codon of *DaMYB75* and *DaMYB56* were individually cloned into the pSPYNE vector. The full-length coding sequences without the stop codon of *DabHLH32* and *DabHLH72* were individually cloned into the pSPYCE vector for Agrobacterium-mediated co-infiltration of *N. benthamiana* leaves as described by Xu et al. [52]. The pSPYNE-AtSPT + pSPYCE-AtIND construct pair was used as a positive control. GFP fluorescence was observed under a FV3000 laser-scanning confocal microscope (Olympus, Tokyo, Japan) 3 days after infiltration. Primers used to generate the constructs used for the BiFC assay are listed in Table S3.

2.11. Yeast one-hybrid (Y1H) assay

To identify regulators of *DaANS* and *DaUFGT* transcription via Y1H assays, promoter fragments (~300 bp long) for each gene of pp about were amplified. Each promoter segment was individually cloned into the pAbAi bait vector; independently, the full-length coding sequences of *DaMYB75*, *DaMYB56*, and *DabHLH72* were individually cloned into the pGADT7 prey vector. The bait plasmids were individually introduced into yeast strain Y1H Gold; positive transformants were selected for growth on synthetic defined (SD) medium lacking uracil (SD/−Ura) medium and used to determine the minimum inhibitory concentration of Aureobasidin A (AbA). Yeast cells harboring each pAbAi plasmid were transformed with

each prey vector, and the positive transformants were selected after 3–4 d of incubation on SD medium lacking leucine (SD/−Leu) at 29 °C. Positive colonies were spotted onto SD/−Leu medium containing the appropriate AbA concentration and incubated at 29 °C for 3–4 d to assess the interactions. The pGADT7 vector and the bait plasmid pAbAi-*proDaANS (S1)*, pAbAi-*proDaANS (S2)*, pAbAi-*proDaUFGT (S1)*, or pAbAi-*proDaUFGT (S2)* were co-transformed as negative controls. The primers used for cloning for the Y1H assays are shown in Table S3.

2.12. Dual-luciferase reporter assay

The full-length coding sequences of *DaMYB75*, *DaMYB56*, and *DabHLH72* were individually cloned into the pGreenII 62-SK vector to generate effector constructs. The promoter fragments *proDaANS (S1)*, *proDaANS (S2)*, *proDaUFGT (S1)*, and *proDaUFGT (S2)* were individually cloned into the pGreenII 0800-LUC vector to produce the reporter constructs. All effector and reporter constructs were individually introduced into Agrobacterium (strain GV3101 with pSoup-19). Positive Agrobacterium colonies were resuspended in infiltration buffer and mixed in the appropriate pairs at a 9:1 ratio (v/v) before being co-infiltrated into *N. benthamiana* leaves as described previously [53]. The ratio of firefly luciferase (LUC)/*Renilla* luciferase (REN) activity was assessed 2 d after infiltration using aDual-Luciferase Reporter Gene Assay Kit according to the manufacturer's instructions (11402ES60, Yeasen, Shanghai, China) on a SpectraMax M2 multimode microplate reader (Molecular Devices, San Jose, CA, USA). The primers used to clone the constructs employed for the dual-luciferase reporter assay are listed in Table S3.

2.13. Electrophoretic mobility shift assay (EMSA)

For EMSA, the full-length coding sequence of *DaMYB75* was cloned into the pDONR207 entry vector (Invitrogen) using the Gateway system, followed by site-specific recombination into the pHMGWA expression vector [54]. The resulting *MBP-DaMYB75* plasmid was introduced into *E. coli* strain BL21, and protein production was induced by adding 0.5 mmol L^{-1} IPTG and incubating at 16 °C for 16 h. The recombinant protein was purified and used for EMSA using a LightShift Chemiluminescent EMSA Kit (Pierce Biotechnology, Rockford, IL, USA) according to the manufacturer's protocol (GE Healthcare Bio-Sciences, Buckinghamshire, UK). Biotin-labeled DNA probes containing either the wild-type (5′-CTTGCCACAGTTGTATGGCA-3′) or mutated MYB-binding site (MBS) sequences and their corresponding competitor DNA were synthesized by Shanghai Sangon Biotechnology (Shanghai, China) based on the *DaANS* promoter sequence. The probes were incubated with 6 μL of the recombinant protein in a 20 μL reaction, with or without the competitor DNA (10×, 20× and 50× excess), for 30 min at room temperature. The entire reaction mixture was separated in a non-denaturing 0.5× TBE 6% polyacrylamide gel for 1 h at 60 V at 4 °C and transferred onto a Biodyne B nylon membrane (Pall Corporation). Signals were visualized with reagents included in the kit using a ChemiDoc XRS system (Bio-Rad Laboratories, Hercules, CA, USA).

3. Results

3.1. Flavonoid composition and contents in D. alata tubers

To explore the mechanisms behind anthocyanin accumulation in *D. alata*, we measured anthocyanin contents in the tubers of three *D. alata* cultivars with contrasting coloration. We detected anthocyanins in the tubers of the pure purple cultivar (Ganzishi 2, pp) and of the faint purple cultivar (Ganziyun 1, fp), in contrast to the very low levels measured in the pure white cultivar (Ganbaiyu 1, pw). The pp and fp tubers showed higher anthocyanin contents at the early stages of tuber formation (120 and 135 DAP), which then declined from 150 d onward (Fig. 1A, B). An analysis of flavonoid-type metabolites at 135 d (pp2, fp2, and pw2) and 180 d (pp5, fp5, and pw5) detected 122 metabolites, six of which belong to the anthocyanin biosynthesis pathway, in *D. alata* tubers (Fig. 1C–E; Table S4). These included three upstream metabolites in the anthocyanin biosynthesis pathway: naringenin, dihydrokaempferol, and dihydroquercetin. The highest levels of these three metabolites were observed in pw tubers, whereas pp and fp tubers generally accumulated similar, lower levels of these metabolites at the same developmental stages (Fig. 1C). The downstream metabolites of the anthocyanin biosynthesis pathway, catechin and epicatechin, were found in lower concentrations in pp tubers compared to pw or fp tubers, particularly at 135 DAP (Fig. 1D). Furthermore, the anthocyanin cyanidin-3-*O*-(2′′-*O*-glucosyl) glucoside exhibited the greatest differential abundance in pp2 tubers relative to pw2 tubers (Fig. 1E), reaching a $\log_2$(fold change) value of 17.2 (Fig. 1F). Notably, pw tubers were richer in flavonols than tubers from the pp and fp cultivars (Tables S5, S6). Kyoto Encyclopedia of Genes and Genomes (KEGG) pathway analysis revealed that the differentially abundant metabolites in pw2 and pp2 were enriched in pathways involved in the biosynthesis of flavones and flavonols, isoflavonoids, and anthocyanins (Fig. 1G).

3.2. Identification of key genes involved in anthocyanin biosynthesis in D. alata

To elucidate the transcriptome landscape of tuber development and coloration in *D. alata*, we performed a transcriptome deep sequencing (RNA-seq) analysis of tubers from the *D. alata* pp, pf, and pw cultivars sampled at 135 and 180 DAP. By comparing transcriptome data from different varieties, we identified differentially expressed genes (DEGs) using the criteria of $|\log_2(\text{fold change})| \geq 1$ and false discovery rate (FDR) < 0.05. Five unigenes showed the highest expression levels in pp2 compared to all other samples: *DaCHS1* (Dioal.17G105700.v2.1), *DaCHI1* (Dioal.09G071500.v2.1), *DaF3′H* (Dioal.13G018200.v2.1), *DaANS* (Dioal.04G138500.v2.1) and *DaUFGT* (Dioal.16G051500.v2.1). Four additional unigenes were most highly expressed in pw2 compared to the other samples: *DaCHS2* (Dioal.17G106700.v2.1), *DaCHI2* (Dioal.19G120300.v2.1), *DaLAR* (Dioal.19G048600.v2.1), and *DaANR* (Dioal.19G053900.v2.1) (Fig. 2).

To investigate the gene regulatory network underlying anthocyanin biosynthesis in *Dioscorea alata*, we conducted weighted gene co-expression network analysis (WGCNA) using transcriptomic and metabolomic data from three cultivars exhibiting the most pronounced divergence in metabolite accumulation at 135 DAP. Genes in the yellow module exhibited a strong positive correlation with anthocyanin contents ($r > 0.8$ and $0 < P < 0.05$) (Fig. S1A). In the yellow module, the expression levels of 41 genes were highly and positively correlated with the levels of cyanidin-3-*O*-(2′′-*O*-glucosyl) glucoside (with edge weight ≥ 0.5). The yellow module consisted of 29 transcription factor genes (2 AP2/ERF genes, 5 bHLH genes, 2 bZIP genes, 3 MADS-box genes, 6 MYB genes, 4 NAC genes, and 7 WRKY genes) and 10 structural genes (Fig. S1B; Table S7). Among these, the expression levels of the LBGs Dioal.04G138500.v2.1 (designated *DaANS*) and Dioal.16G051500.v2.1 (designated *DaUFGT*) were positively correlated with the content of cyanidin-3-*O*-(2′′-*O*-glucosyl) glucoside, suggesting that *DaANS* and *DaUFGT* are the structural genes responsible for anthocyanin biosynthesis in the *D. alata* cultivar with pure purple tubers. Similar analysis revealed that proanthocyanidins contents showed a strong positive correlation with the expression levels of genes

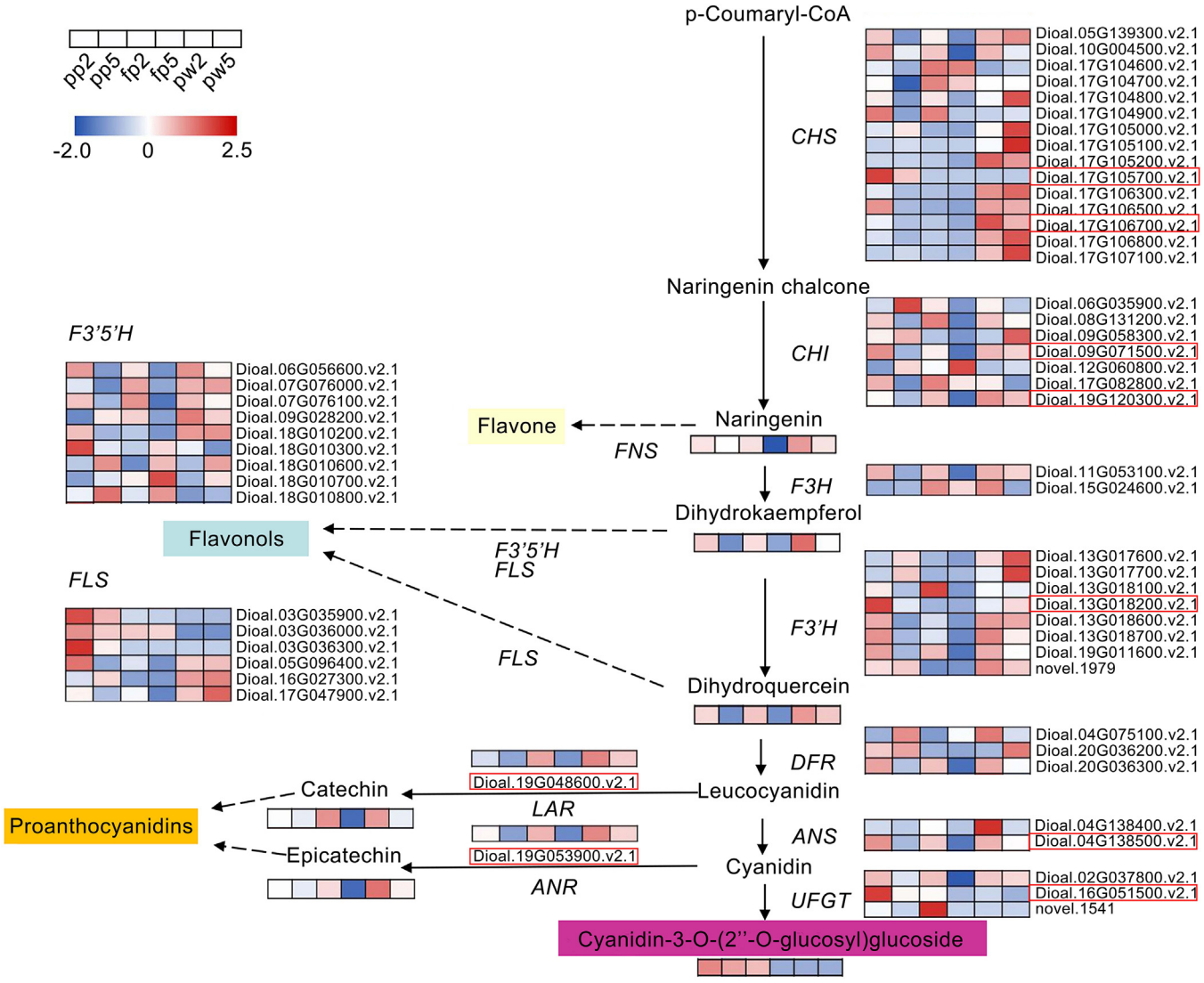

Fig. 2. Metabolic flux through the flavonoid biosynthetic pathway and transcriptome profiles of the related *D. alata* structural genes. pp2, fp2, and pw2 indicate 135 d after planting; pp5, fp5, and pw5 indicate 180 d after planting. Red indicates high expression or high metabolite content, and blue represents low expression or low metabolite content. The heatmaps were plotted using $\log_2$-transformed relative metabolite contents and FPKM values. The gene IDs of potential DEGs are highlighted in red boxes.

from the red and turquoise modules ($r > 0.8$ and $0 < P < 0.05$) (Fig. S1A). We identified 60 and 18 genes, respectively, in the turquoise and red modules (Tables S8, S9).

As MYB-type transcription factors typically contribute to anthocyanin biosynthesis in plants, we looked for all R2R3-MYB genes in the *D. alata* genome, yielding 97 members (Table S10). We reconstructed a maximum-likelihood phylogenetic tree using these 97 R2R3-DaMYBs and the 126 R2R3-MYBs from Arabidopsis. These R2R3-MYB genes were divided into 23 subgroups, with two *D. alata* genes (Dioal.15G115700.1.v2.1 and Dioal.15G116900.1.v2.1) belonging to subgroup S6 related to anthocyanin biosynthesis (Fig. S2A). Only Dioal.15G115700.v2.1 (renamed *DaMYB75*) was part of the yellow module and was co-expressed with *DaANS* and *DaUFGT* (Table S7). Phylogenetic analysis revealed that DaMYB75 was grouped with S6 subfamily members (Fig. S2B). Multiple sequence alignment between DaMYB75 and related S6-subgroup proteins revealed conserved R2 and R3 domains in the N-terminus of the protein, including a conserved interaction motif with bHLH transcription factors and an ANDV motif. These motifs, which are present in the R3 domains of MYB transcription factors, promote anthocyanin accumulation in dicots, as does the SG6 motif, which is also present in DaMYB75 (Fig. S2C) [55,56].

A similar search for bHLH genes in the *D. alata* genome returned a total of 100 bHLH transcription factor genes (Table S11), with three bHLH genes (Dioal.06G066200.v2.1, Dioal.14G025100.v2.1, and Dioal.19G165800.v2.1) belonging to the IIIf subgroup based on phylogenetic analysis (Fig. S3A). Among these, Dioal.06G066200.v2.1 (renamed *DabHLH32*) was co-expressed with *DaANS* and *DaUFGT* (Table S7). Furthermore, Dioal.14G025100.v2.1 (renamed *DabHLH72*) was identified as a candidate gene related to proanthocyanidin biosynthesis, as its expression levels were positively correlated with proanthocyanidin levels in the turquoise module (Table S8). Previous studies have revealed that IIIf subgroup bHLH transcription factors simultaneously regulate anthocyanin biosynthesis, proanthocyanidin biosynthesis, and trichome initiation in other plant species, such as *Chimonanthus praecox*, *Narcissus tazetta*, and *Freesia hybrida* [57–59]. Therefore, DabHLH72 may regulate both proanthocyanin and anthocyanin biosynthesis in *D. alata*.

Phylogenetic analysis revealed that DabHLH32 and DabHLH72 are located in the GLABRA 3 (GL3) and TRANSPARENT TESTA 8 (TT8) clades, respectively, of the IIIf subgroup (Fig. S3B). Multiple amino acid sequence alignment highlighted the presence of three conserved domains in DabHLH32 and DabHLH72: an N-terminal

MYB interaction region (MIR), a bHLH domain, and a putative ACT-like domain at the C-terminus. The MIR is responsible for protein–protein interactions between MYB transcription factors, whereas the ACT-like domain participates in dimerization (Fig. S3C). Importantly, *DaANS*, *DaUFGT*, and *DaMYB75* were generally highly expressed in anthocyanin-rich tissues, whereas *DabHLH32* showed expression patterns consistent with anthocyanin levels only in specific tissues (including roots, tender leaves, epidermis, and tuber fleshes) of pp and fp at 135 DAP, but exhibited higher expression levels in pw tissues. *DabHLH72* was expressed at higher levels in most tissues of pw compared to pp and fp (Fig. S4A–L). We assessed the subcellular localizations of the transcription factors DaMYB75, DaMYB56, DabHLH32, and DabHLH72 by cloning their-coding sequences in-frame and upstream of the green fluorescent protein (*GFP*) gene and infiltrating the resulting constructs into the leaves of *N. benthamiana* plants. We detected green fluorescence in the nucleus for all tested constructs, indicating that these transcription factors are nuclear proteins (Fig. S4M).

3.3. The DaMYB75-DabHLH72 interaction strongly promotes anthocyanin accumulation

To investigate the contributions of DaMYB75 and DabHLH72 to anthocyanin accumulation, we heterologously overexpressed each gene in tobacco (*N. tabacum*) cultivar K326 Compared to the wild type (WT), the leaves and flowers of *DaMYB75* overexpression lines (OE-12 and OE-14) showed prominent pigment accumulation (Fig. 3A). *DaMYB75* was highly expressed in the transgenic lines (Fig. 3B), which contained considerably more anthocyanins in their leaves and flowers than the WT (Fig. 3C). Additionally, the expression of anthocyanin biosynthesis–related genes was markedly induced in the leaves and flowers of the transgenic lines relative to the WT (Fig. S5A). To extend these results to *D. alata*, we overexpressed *DaMYB75* in pw leaves and conducted VIGS-mediated silencing of *DaMYB75* in pp tubers. Compared to plants infiltrated with the respective empty vector (as a control), the anthocyanin contents and *DaANS* and *DaUFGT* expression levels significantly increased in the leaves of pw plants overexpressing *DaMYB75* (Fig. 3D–G). In addition, silencing *DaMYB75* expression in the pp cultivar background resulted in lower *DaMYB75* transcript levels and anthocyanin levels, resulting in the diminished purple coloration of tubers around the infiltration sites (Fig. 3H–J). In these infiltrated tubers, the expression levels of *DaANS* and *DaUFGT* were lower than in tubers infiltrated with the empty pTRV construct (Fig. 3K, L). We conclude that DaMYB75 promotes anthocyanin biosynthesis and accumulation in tobacco and *D. alata*.

As MYBs form MBW complexes with bHLH family to modulate anthocyanin accumulation in plants, we tested the interaction potential of DaMYB75 with DabHLH32 and DabHLH72. Indeed, DaMYB75 weakly interacted with DabHLH32, whereas DaMYB75 interacted strongly with DabHLH72, in yeast two-hybrid (Y2H) assays (Fig. 3M). In a bimolecular fluorescence complementation (BiFC) assay in *N. benthamiana* leaves, DaMYB75 interacted with DabHLH72, but not with DabHLH32 (Fig. 3N). To assess the combined functions of DaMYBs and DabHLHs in anthocyanin biosynthesis, we infiltrated *N. benthamiana* leaves with constructs expressing *DaMYB75*, *DabHLH32*, or *DabHLH72* or co-infiltrated leaves with constructs expressing *DaMYB75* along with *DabHLH32* or *DabHLH72*. One week later, we observed pigment accumulation only in leaves co-infiltrated with *DaMYB75* and *DabHLH72*. After two weeks, *DaMYB75* expression was sufficient for anthocyanin accumulation, which was nevertheless enhanced when *DabHLH32* or *DabHLH72* was co-expressed with *DaMYB75* (Fig. S6A).

To confirm the anthocyanin accumulation in *N. benthamiana* leaves based on visible observation, we measured anthocyanin contents and the expression levels of the related structural genes. No anthocyanin accumulation and no expression of structural genes resulted from the heterologous expression of *DabHLH32* or *DabHLH72* alone (Fig. S6B, C). We obtained largely similar results when we infiltrated or co-infiltrated the same constructs in the leaves of the *D. alata* pw cultivar: co-expressing *DaMYB75* and *DabHLH72* produced leaf sectors with a deep purple color and high anthocyanins levels one week after co-infiltration; co-infiltrating *DaMYB75* and the empty vector led to anthocyanin accumulation, although to a lesser extent (Fig. 3O, P). In agreement with these results, we noted a significant rise in *DaANS* and *DaUFGT* expression levels following co-infiltration with *DaMYB75* and *DabHLH72* compared to *DaMYB75* and the empty vector control (Fig. 3Q, R). The leaves of the *D. alata* pw cultivar also accumulated anthocyanins when co-infiltrated with *DaMYB75* and the empty vector or *DabHLH32*, with no synergistic effects observed between DaMYB75 and DabHLH32. Indeed, anthocyanin levels and the expression levels of *DaANS* and *DaUFGT* were relatively high when *DaMYB75* was overexpressed, regardless of whether DabHLH32 was present (Fig. S7).

3.4. The DaMYB75–DabHLH72 interaction activates transcription from the DaANS promoter

We took a closer look at the *DaANS* and *DaUFGT* promoter sequences, which revealed one MYB-binding site and three bHLH-binding sites in the *DaANS* promoter (Fig. S8) and three bHLH-binding sites in the *DaUFGT* promoter (Fig. S9). We cloned two ~300-bp segments of each promoter containing the MYB or bHLH sites into the pAbA vector for a yeast one-hybrid (Y1H) assay, yielding the plasmids *proDaANS (S1)*, *proDaANS (S2)*, *proDaUFGT (S1)*, and *proDaUFGT (S2)* (Fig. 4A). DaMYB75 bound to the *proDaANS (S2)* segment, which contained an MYB-binding site, whereas DabHLH72 failed to bind to any of these four promoter segments (Fig. 4B). We designed a probe containing the MYB-binding site in the *DaANS* promoter for use in an electrophoretic mobility shift assay (EMSA). Recombinant purified maltose-binding protein (MBP)-DaMYB75 bound to the probe containing the MYB-binding site (Fig. 4C). To assess the consequences of DaMYB75 binding to the *DaANS* promoter on transcription, we performed a dual-luciferase reporter assay in *N. benthamiana* leaves. Although expressing *DabHLH72* did not activate transcription from the *proDaANS (S1)*, *proDaANS (S2)*, *proDaUFGT (S1)*, or *proDaUFGT (S2)* segments over the levels seen with the empty control, expressing *DaMYB75* resulted in higher relative firefly luciferase activity from the *proDaANS (S2)* segment, which was further enhanced in the presence of DabHLH72 (Fig. 4D). These results suggest that DaMYB75 binds to the MYB-binding site of the *DaANS* promoter to induce its transcription, with DabHLH72 promoting the transcriptional activation activity of DaMYB75.

3.5. Measuring DNA methylation levels at the DaMYB75 promoter

To investigate possible natural variation among structural and/or regulatory genes related to anthocyanin biosynthesis in *D. alata*, we cloned the coding sequences and the promoters of the key structural gene *DaANS* from the pp and pw cultivars (Table S12). There was a single amino acid difference in DaANS between the pp and pw cultivars at the penultimate amino acid, which did not affect the conserved functional domains of DaANS (Fig. S10A). Multiple sequence alignment between the two DaANS variants and ANS proteins from other plant species revealed the conservation of amino acids in the active site (His-236, Asp-238, His-292, Arg-302, and Ser-304) and the binding site (Glu234) (Fig. S10B), suggesting that DaANS might perform a similar function to ANS in other species. Compared to pp, the *DaANS* promoter sequence in pw differed at six locations in the first 450 bp

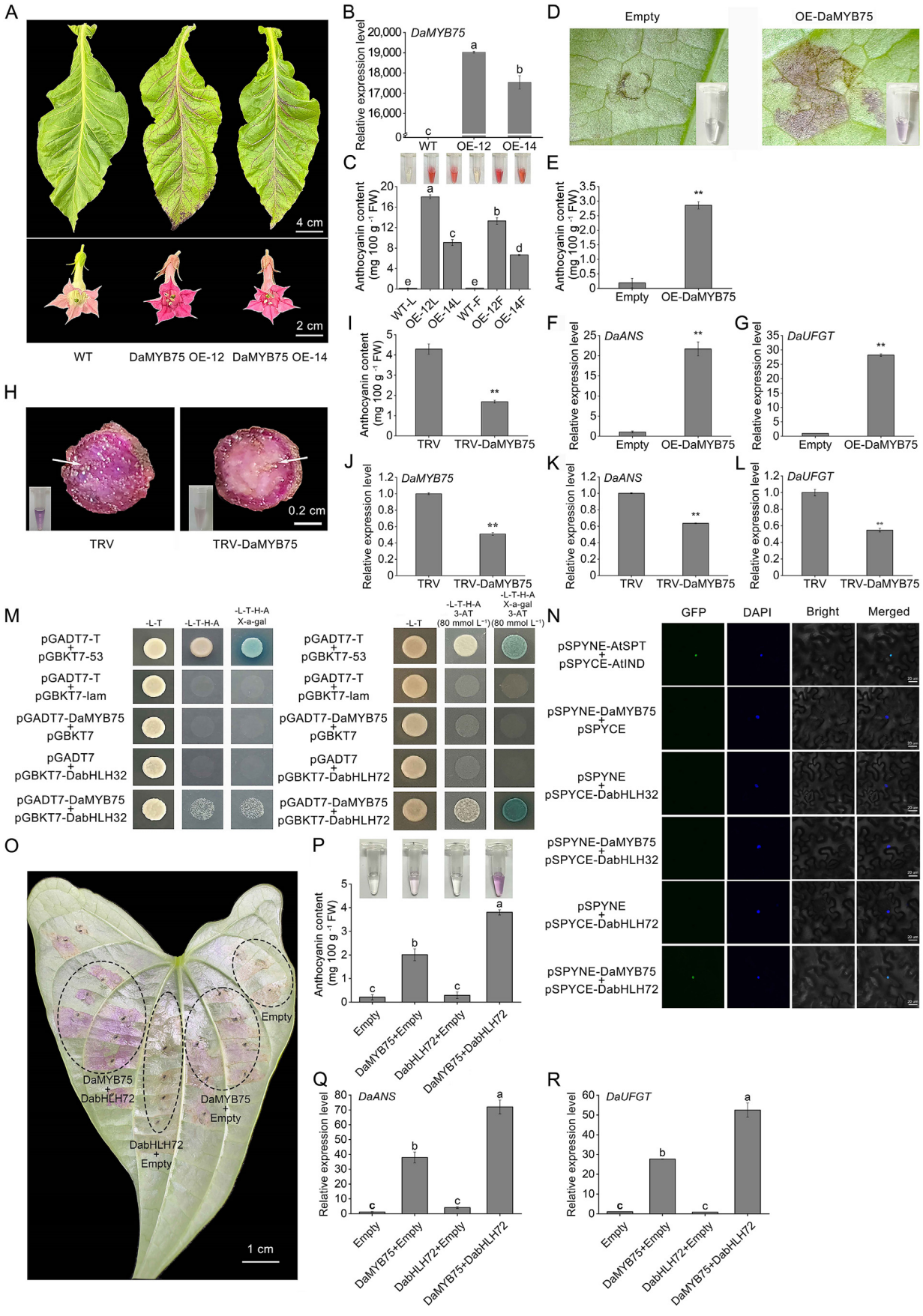
A
4 cm
2 cm
WT
DaMYB75 OE-12
DaMYB75 OE-14
B
DaMYB75
Relative expression level
WT
OE-12
OE-14
C
Anthocyanin content (mg 100 g⁻¹ FW)
WT-L
OE-12L
OE-14L
WT-F
OE-12F
OE-14F
D
Empty
OE-DaMYB75
E
Anthocyanin content (mg 100 g⁻¹ FW)
Empty
OE-DaMYB75
F
DaANS
Relative expression level
G
DaUFGT
Relative expression level
H
0.2 cm
TRV
TRV-DaMYB75
I
Anthocyanin content (mg 100 g⁻¹ FW)
J
DaMYB75
Relative expression level
K
DaANS
Relative expression level
L
DaUFGT
Relative expression level
M
-L-T
-L-T-H-A
-L-T-H-A X-a-gal
-L-T-H-A 3-AT (80 mmol L⁻¹)
-L-T-H-A X-a-gal 3-AT (80 mmol L⁻¹)
pGADT7-T + pGBKT7-53
pGADT7-T + pGBKT7-lam
pGADT7-DaMYB75 + pGBKT7
pGADT7 + pGBKT7-DabHLH32
pGADT7-DaMYB75 + pGBKT7-DabHLH32
pGADT7 + pGBKT7-DabHLH72
pGADT7-DaMYB75 + pGBKT7-DabHLH72
N
GFP
DAPI
Bright
Merged
pSPYNE-AtSPT + pSPYCE-AtIND
pSPYNE-DaMYB75 + pSPYCE
pSPYNE + pSPYCE-DabHLH32
pSPYNE-DaMYB75 + pSPYCE-DabHLH32
pSPYNE + pSPYCE-DabHLH72
pSPYNE-DaMYB75 + pSPYCE-DabHLH72
O
Empty
DaMYB75 + DabHLH72
DaMYB75 + Empty
DabHLH72 + Empty
1 cm
P
Anthocyanin content (mg 100 g⁻¹ FW)
Empty
DaMYB75+Empty
DabHLH72+Empty
DaMYB75+DabHLH72
Q
DaANS
Relative expression level
R
DaUFGT
Relative expression level

upstream of the translation start site, with one 1-bp insertion, one 4-bp insertion, one 5-bp insertion, and three single-base substitutions. We cloned the *DaANS* promoter sequences from two *D. alata* cultivars with pure purple tuber flesh (Yichun purple yam and Guangzhou purple yam) and two *D. alata* cultivars with pure white tuber flesh (Qujiang white yam and Longnan white yam), finding that Yichun purple yam (with pure purple tubers) carried a *DaANS* promoter sequence identical to that of the pw cultivar (Figs. S11, S12; Table S12).

Similarly, the amino acid sequence of DaMYB75 was identical in the pp and pw cultivars. There was only a 1-bp deletion in the *DaMYB75* promoter in the pw cultivar (Fig. S13). However, the sequence of the *DaMYB75* promoter in the pp cultivar was the same as for the other cultivars, Qujiang white yam and Longnan white yam, both with pure white tubers (Table S12). We measured the cytosine methylation levels over four *DaMYB75* promoter fragments in the pp and pw cultivars by bisulfite sequencing PCR (BSP) (Fig. S14). The regions from −1214 bp to −988 bp and from −1561 bp to −1300 bp showed pronounced differences in methylation levels between pp and pw (Fig. 5A, B). In pw, 20.7% and 71.1% of all cytosines were methylated in the −1561 bp to −1300 bp and −1214 bp to −988 bp regions, respectively, in contrast to only 1.3% and 57.6% in pp, respectively. The methylation levels in the CG and CHG (H = A, C, or T) contexts at the *DaMYB75* promoter in the −1561 bp to −1300 bp segment showed a striking difference between pw and pp, with methylation levels in the CG and CHG contexts of 93.9% and 97.2% in pw, respectively, whereas no methylation was detected in pp (Fig. 5C). In the region from −1214 bp to −988 bp, the methylation levels in the CG and CHG contexts in pw were 57.2% and 50.2% higher than those in pp, respectively (Fig. 5D). Therefore, DNA methylation along the *DaMYB75* promoter might be associated with the low *DaMYB75* expression in the *D. alata* cultivar with pure white tubers.

3.6. DaMYB56 inhibits DaANS transcription by interacting with DabHLH72

We identified six members of the S4 subgroup R2R3-MYB transcription factor family. Based on our RNA-seq data, Dioal.11G046900.v2.1 (renamed *DaMYB56*) expression exhibited differences between the pp and pw cultivars (Fig. S15A). We observed a significant increase in *DaMYB56* expression levels in the stems, epidermis and flesh from pp tubers at 180 DAP, along with low anthocyanin contents compared to other tissues with high anthocyanin contents (Fig. 6A, B). Phylogenetic analysis indicated that DaMYB56 clustered with other members of the AtMYB4-like clade, which comprises known R2R3-MYB repressors of anthocyanin accumulation (Fig. S15B). DaMYB56 contains a bHLH-binding motif, as determined by amino acid sequence alignment, and an EAR motif, which is present in transcriptional repressors (Fig. S15C). DaMYB56-GFP fusion protein localized to the nucleus (Fig. S4M). To assess DaMYB56 function, we generated transgenic tobacco plants heterologously overexpressing *DaMYB56*: compared to the light pink flowers of the nontransgenic WT, the flowers of the *DaMYB56* transgenic plants (OE-1 and OE-5) showed visible phenotypic changes, turning almost white. In agreement with this observation, the transgenic plants accumulated significantly lower levels of anthocyanins and displayed the downregulation of anthocyanin biosynthetic genes compared to WT (Figs. 6C, D, S5B).

We determined that DaMYB56 interacts with DabHLH72 in Y2H and BiFC assays (Fig. 6E, F). To test the possible role of DaMYB56 in anthocyanin accumulation, we co-infiltrated the leaves of the *D. alata* pw cultivar with *DaMYB75*, *DabHLH72*, and the empty vector, yielding purple pigmentation in the infiltrated leaf sectors one week later. Importantly, the pigmentation of the leaf sector co-infiltrated with *DaMYB75*, *DabHLH72*, and *DaMYB56* was very modest (Fig. 6G). Consistent with this result, the anthocyanin content and the expression levels of the key anthocyanin biosynthesis gene *DaANS* were significantly higher in *D. alata* pw leaves co-infiltrated with *DaMYB75*, *DabHLH72*, and the empty vector than in leaves co-infiltrated with *DaMYB75*, *DabHLH72*, and *DaMYB56* (Fig. 6H, I). Y1H assays showed that DaMYB56 binds to the pAbAi-*proDaANS (S2)* promoter fragment (Fig. 6J). To assess the effect of DaMYB56 binding on transcription, we performed a dual-luciferase reporter assay with a *proDaANS(S2):LUC* reporter construct in *N. benthamiana* leaves. Whereas co-infiltrating the reporter construct with *DaMYB75*, and *DabHLH72* led to high relative LUC activity, the presence of DaMYB56 abolished the transcriptional activation of the reporter (Fig. 6K). We conclude that DaMYB56 represses the transcriptional activation mediated by DaMYB75.

4. Discussion

4.1. DaMYB75 and DabHLH72 synergistically promote anthocyanin biosynthesis by activating transcription from the DaANS promoter

Anthocyanins are widely distributed in plants and are important for the appearance and quality characteristics of many horticultural crops [3,60]. The most prevalent types of anthocyanin aglycones in horticultural plants are malvidin, pelargonidin, petunidin, peonidin, delphinidin, and cyanidin [61]. The major anthocyanins that accumulate in *D. alata* cultivars with purple tubers are cyanidin derivatives, including cyanidin 3-(6-sinapoyl

Fig. 3. DaMYB75 interacts with DabHLH72 to promote anthocyanin accumulation. (A) Representative photographs of leaves (top) and flowers (bottom) of wild-type (WT) tobacco (cultivar K326) plants and transgenic lines overexpressing *DaMYB75* (OE-12 and OE-14). Scale bars, 4 cm (top), 2 cm (bottom). (B) Relative *DaMYB75* expression in WT and *DaMYB75*-OE lines, as determined by RT-qPCR. (C) Total anthocyanin contents in WT and *DaMYB75*-OE tobacco plants. (D) Results of infiltrating the empty vector or the *DaMYB75*-OE construct in the leaves of the pw *D. alata* cultivar. (E-G) Total anthocyanin contents (E) and relative expression levels of *DaANS* (F) and *DaUFGT* (G) in leaf sectors infiltrated with the empty vector or the *DaMYB75*-OE construct in the leaves of the pw *D. alata* cultivar. (H, I) Representative photographs (H) and total anthocyanin contents (I) of *D. alata* tubers infiltrated with the empty pTRV vector (TRV) or the *DaMYB75* silencing construct (TRV-*DaMYB75*). (J–L) Relative transcript levels of *DaMYB75* (J), *DaANS* (K), and *DaUFGT* (L) in *D. alata* tubers infiltrated with TRV or TRV-*DaMYB75*. (M) Yeast two-hybrid (Y2H) assay testing the interaction between DaMYB75 and DabHLH32 or DabHLH72. pGBKT7-53 + pGADT7-T was used as a positive control and pGBKT7-lam + pGADT7-T as a negative control. –T–L: synthetic defined (SD) medium lacking Trp and Leu; –T–L–H –A: SD medium lacking Trp, Leu, His, and Ade. 3-AT and X-α-gal were added as an inhibitor and chromogenic substrate, respectively. (N) Bimolecular fluorescence complementation (BiFC) assays in *N. benthamiana* leaves. *DaMYB75* was cloned into the pSPYNE vector, whereas *DabHLH32* or *DabHLH72* was cloned into the pSPYCE vector. pSPYNE-*AtSPT* + pSPYCE-*AtIND* was used as a positive control. Nuclei were stained with DAPI. Scale bars, 20 μm. (O) Representative photograph of a *D. alata* leaf co-infiltrated with *35S:DaMYB75* and/or *35S:DabHLH72*. (P) Total anthocyanins contents in *D. alata* leaves co-infiltrated with the indicated constructs. (Q, R) Relative expression levels of *DaANS* (Q) and *DaUFGT* (R) in *D. alata* leaves co-infiltrated with the indicated constructs. FW, fresh weight. In (B, C, E–G, I–L, P–R), values are means ± standard error from three biological replicates. In (B, C, P–R), different lowercase letters indicate significant differences, as determined by one-way ANOVA, with $P < 0.05$. In (E–G, I–L), significant differences between the experimental and control groups were determined by Student's *t*-test (**, $P < 0.01$).

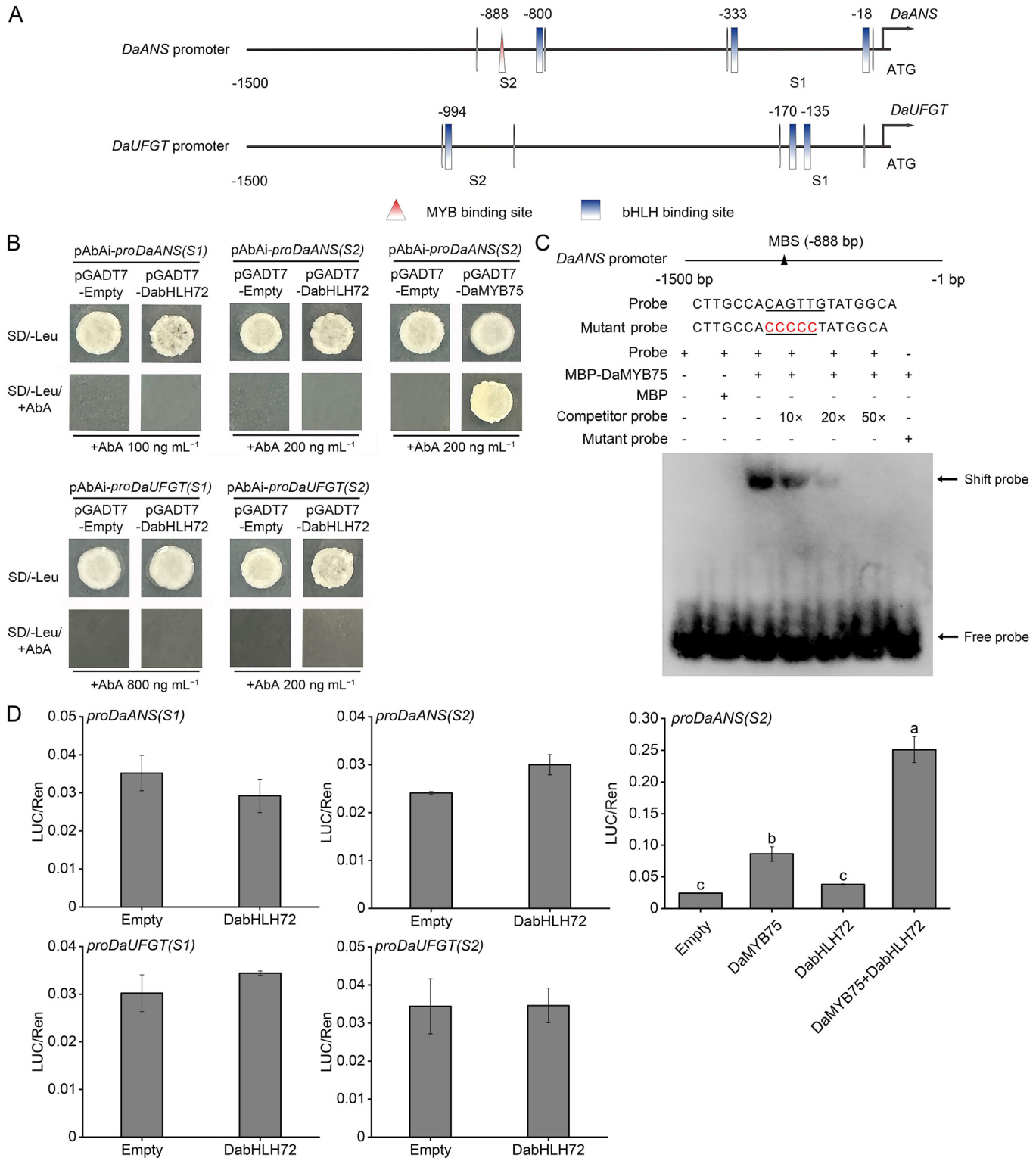

Fig. 4. Evaluation of the *cis*-regulatory sites of the *DaANS* and *DaUFGT* promoters recognized by DaMYB75 and DabHLH72. (A) Diagrams of the *DaANS* and *DaUFGT* promoters. The presence of *cis*-elements was determined using the PlantCare database. Each promoter was divided into two segments, S1 and S2, as indicated by solid vertical lines. (B) Yeast one-hybrid (Y1H) assays testing the binding of DaMYB75 or DabHLH72 to the *DaANS* and *DaUFGT* promoters. SD/−Leu, synthetic defined (SD) medium lacking Leu. Aureobasidin A (AbA) was added as an inhibitor. (C) Electrophoretic mobility shift assay (EMSA) showing the binding of recombinant purified MBP-DaMYB75 to the *DaANS* promoter. Biotin-labeled probes containing specific MYB-binding sites (MBSs) present in the *DaANS* promoter were mixed with MBP-DaMYB75. Unlabeled probes or mutant probes disrupting the MBS served as competitor probes. (D) Dual-luciferase reporter assay in *N. benthamiana* leaves co-infiltrated with the reporter constructs *proDaANS(S1):LUC*, *proDaANS(S2):LUC*, *proDaUFGT(S1):LUC*, or *proDaUFGT(S2):LUC* and the effector constructs *35S:DaMYB75* and/or *35S:DabHLH72*. Values are means ± standard error from three biological replicates. Different lowercase letters indicate significant differences, as determined by a one-way ANOVA, with $P < 0.05$.

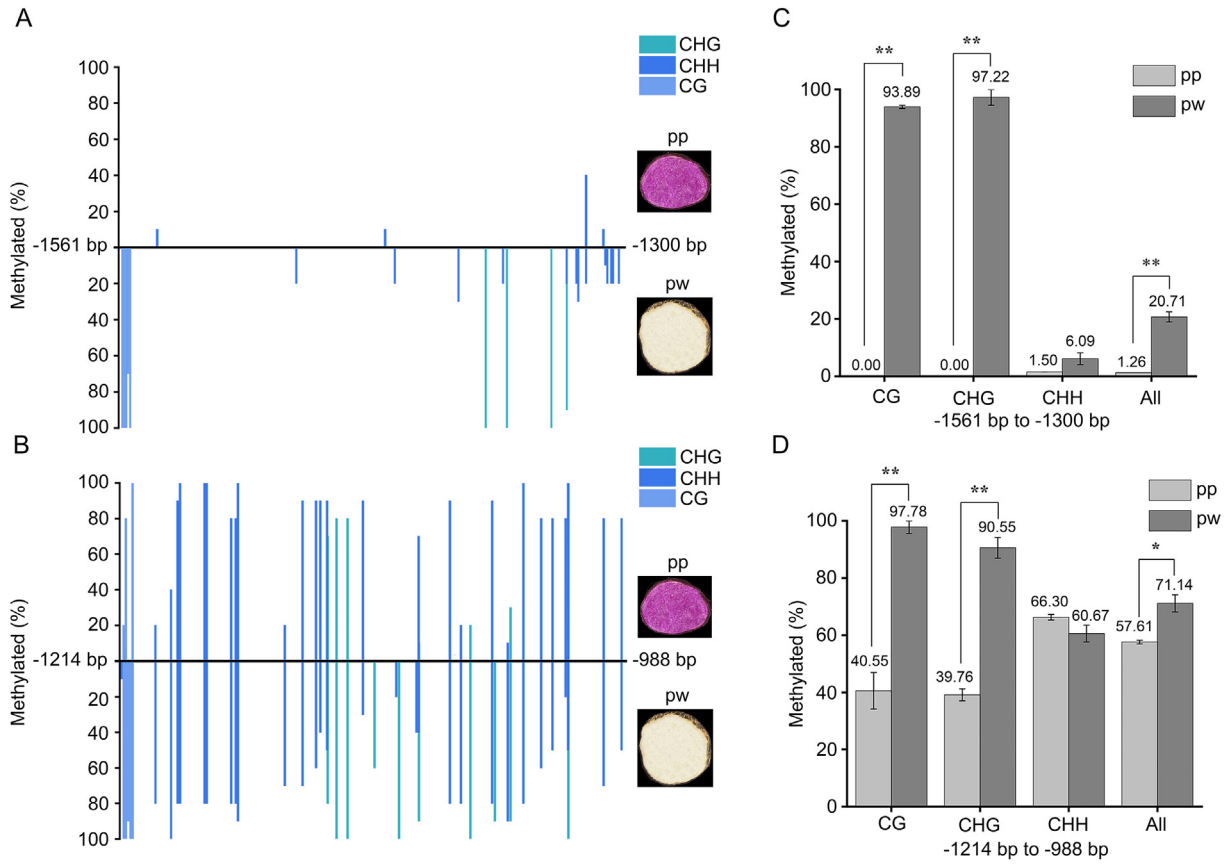

Fig. 5. DNA methylation analysis of the *DaMYB75* promoters in the pp and pw *D. alata* cultivars. (A, B) Bisulfite sequencing PCR analysis of DNA methylation levels along the *DaMYB75* promoter segments from the −1561 bp to −1300 bp (A) and the −1214 bp to −988 bp regions (B) between the pp and pw cultivars. The percentage of methylation at each cytosine is indicated by vertical bars. CG, CHG, and CHH-type cytosine methylations is represented by lines of different colors. (C, D) Percentages of cytosine methylation along the −1561 bp to −1300 bp (C) and −1214 bp to −988 bp regions (D) of the *DaMYB75* promoter in the pp and pw cultivars. Values are means ± standard error from three biological replicates. Significant differences between the experimental and the control groups were determined by Student's *t*-test (*, $P < 0.05$; **, $P < 0.01$).

gentiobioside), cyanidin 3-hexoside acylation, and cyanidin 3-glucoside acylation [62,63]. In this study, we detected high levels of the cyanidin glycoside cyanidin-3-*O*-(2′′-*O*-glucosyl) glucoside in the tubers of the pp cultivar compared to those of the fp and pw cultivars, with the greatest differential accumulation between the pp and pw cultivars observed at 135 DAP.

The anthocyanin biosynthesis pathway in plants is generally well understood, at least in *Arabidopsis* [12]. This pathway consists of a series of enzymes encoded by EBGs and LBGs [5,64]. In the present study, we identified two LBGs (*DaANS* and *DaUFGT*) through WGCNA based on the strong positive correlation of their expression levels with anthocyanin accumulation. Analysis of the spatial and temporal expression patterns of these two genes revealed that *DaANS* and *DaUFGT* are highly expressed in tissues with elevated anthocyanin contents. Besides structural genes, anthocyanin biosynthesis is mainly controlled by transcription factors, with R2R3-MYBs and bHLHs playing major roles in anthocyanin biosynthesis by forming MBW complexes. bHLH3 and MYBA bind directly to the *ANS* promoter in mulberry (*Morus nigra*) fruits, with bHLH3 acting as a key regulator of the MYBA-bHLH3-TTG1 complex [65]. Similarly, CcMYB6-1 induced transcription from the promoters of *CcF3H* and *CcDFR* in cornflower (*Centaurea cyanus*). The promoter activity was further enhanced by the presence of CcbHLH1 [66]. DcTT8 participates in anthocyanin biosynthesis by directly binding to the *DcUFGT* and *DcF3′H* promoters in the orchid *Dendrobium candidum* [67].

In the current study, we identified DaMYB75 from the R2R3-MYB S6 subgroup based on the co-expression of its encoding gene with *DaANS* and *DaUFGT*. We showed that DaMYB75 positively regulates anthocyanin biosynthesis by overexpressing this gene in tobacco and *D. alata*, which led to anthocyanin accumulation. By contrast, silencing *DaMYB75* in the *D. alata* pp cultivar diminished anthocyanin accumulation and *DaANS* and *DaUFGT* expression. As part of a putative MBW complex, we identified two bHLHs (DabHLH32 and DabHLH72) of the IIIf subgroup as regulating anthocyanins biosynthesis in *D. alata*. We established that DaMYB75 and DabHLH72 interact, as determined by Y2H and BiFC assays. Co-expression of *DabHLH72* and *DaMYB75* strongly promoted anthocyanin accumulation in the leaves of *N. benthamiana* and *D. alata* plants, although DabHLH72 alone did not. Y1H, dual-luciferase reporter assays, and EMSA demonstrated that DaMYB75 directly binds to the *DaANS* promoter to activate its transcription, which was further enhanced by the interaction of DaMYB75 with DabHLH72. However, DabHLH72 did not bind to or activate transcription from the *DaANS* or *DaUFGT* promoters. It is likely that DaMYB75 and DabHLH72 form a transcriptional complex that regulates *DaANS* expression, leading to anthocyanin accumulation in *D. alata*. Notably, DabHLH32 did not promote anthocyanin accumulation when expressed in *N. benthamiana* or *D. alata* leaves, nor did it interact with DaMYB75 in Y2H or BiFC assays. As multiple MYBs can regulate anthocyanin biosynthesis in the same plant [68], we suggest that DabHLH32 might interact with MYBs other

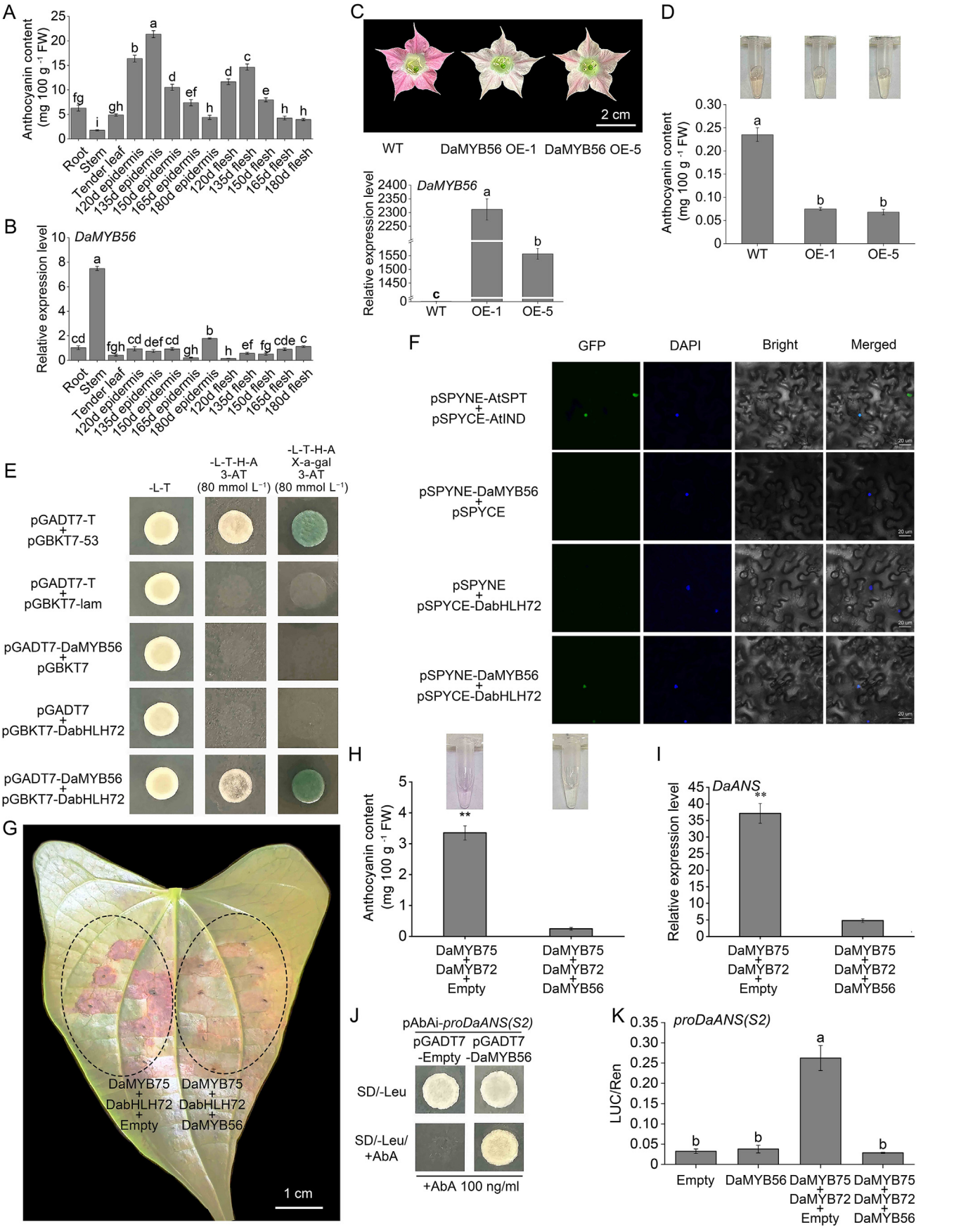
A
Anthocyanin content (mg 100 g -1 FW)
Root
Stem
Tender leaf
120d epidermis
135d epidermis
150d epidermis
165d epidermis
180d epidermis
120d flesh
135d flesh
150d flesh
165d flesh
180d flesh
B
Relative expression level
DaMYB56
C
2 cm
WT
DaMYB56 OE-1
DaMYB56 OE-5
Relative expression level
DaMYB56
D
Anthocyanin content (mg 100 g -1 FW)
WT
OE-1
OE-5
E
-L-T
-L-T-H-A 3-AT (80 mmol L-1)
-L-T-H-A X-a-gal 3-AT (80 mmol L-1)
pGADT7-T + pGBKT7-53
pGADT7-T + pGBKT7-lam
pGADT7-DaMYB56 + pGBKT7
pGADT7 + pGBKT7-DabHLH72
pGADT7-DaMYB56 + pGBKT7-DabHLH72
F
GFP
DAPI
Bright
Merged
pSPYNE-AtSPT + pSPYCE-AtIND
pSPYNE-DaMYB56 + pSPYCE
pSPYNE + pSPYCE-DabHLH72
pSPYNE-DaMYB56 + pSPYCE-DabHLH72
20 um
G
DaMYB75 + DabHLH72 + Empty
DaMYB75 + DabHLH72 + DaMYB56
1 cm
H
Anthocyanin content (mg 100 g -1 FW)
DaMYB75 + DaMYB72 + Empty
DaMYB75 + DaMYB72 + DaMYB56
I
DaANS
Relative expression level
DaMYB75 + DaMYB72 + Empty
DaMYB75 + DaMYB72 + DaMYB56
J
pAbAi-proDaANS(S2)
pGADT7 -Empty
pGADT7 -DaMYB56
SD/-Leu
SD/-Leu/ +AbA
+AbA 100 ng/ml
K
proDaANS(S2)
LUC/Ren
Empty
DaMYB56
DaMYB75 + DaMYB72 + Empty
DaMYB75 + DaMYB72 + DaMYB56

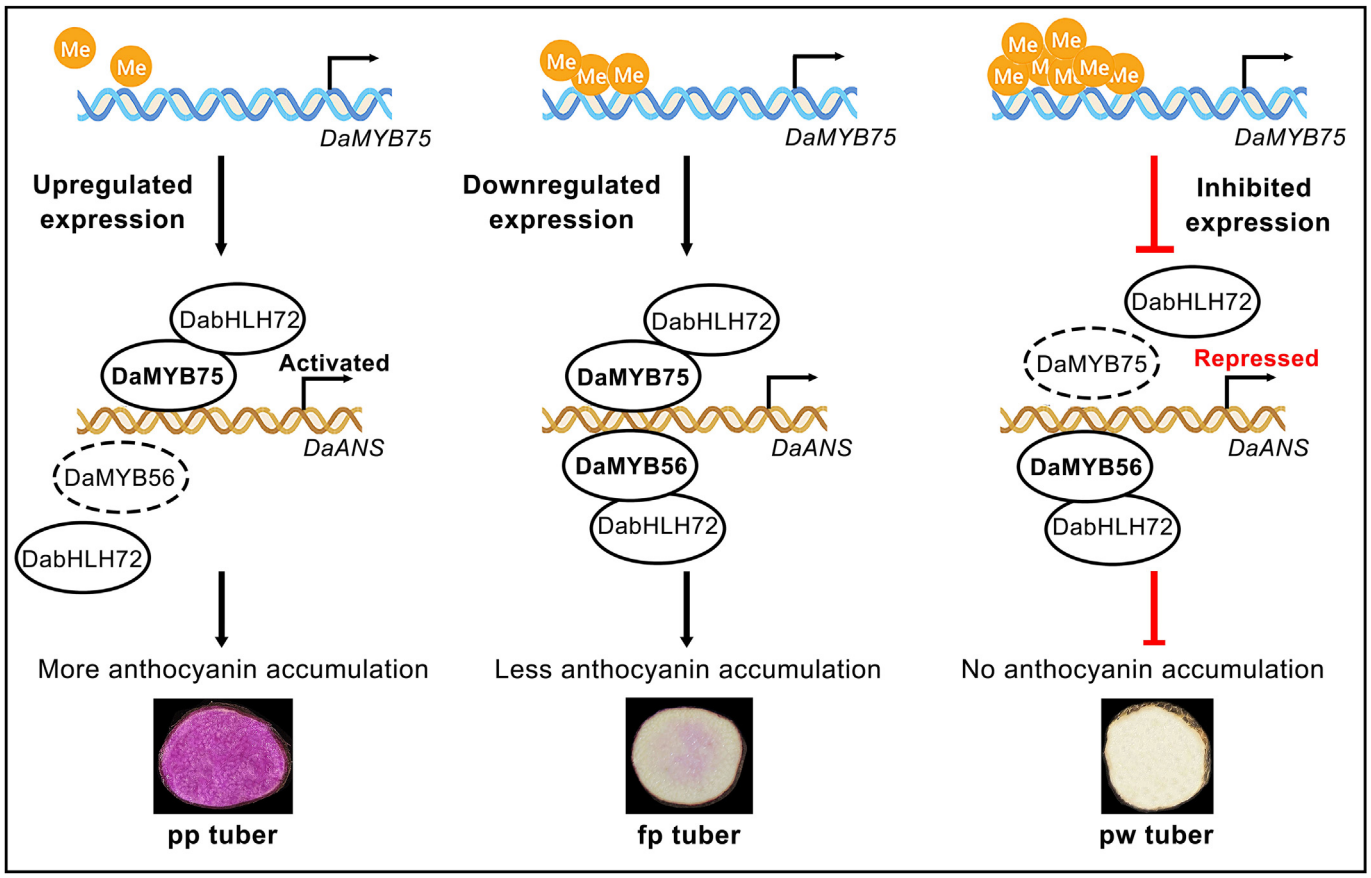

Fig. 7. A model of the potential molecular mechanism behind anthocyanin accumulation in *D. alata* tubers.

than DaMYB75, highlighting the complexity of anthocyanin regulatory networks in *D. alata*.

4.2. DaMYB56 and DabHLH72 synergistically inhibit anthocyanin biosynthesis by binding to the DaANS promoter

R2R3-MYB members of the S4 subfamily are negative regulators of anthocyanin biosynthesis in horticultural plants. For example, MYB182 inhibits anthocyanin biosynthesis in poplar by inhibiting the expression of structural genes related to anthocyanin biosynthesis [32]. PpMYB18 is a negative regulator of anthocyanin and proanthocyanidin accumulation in peach, which competitively binds to PpbHLH3 to PpMYB10.1 to regulate anthocyanin accumulation in fruits [30]. In potato (*Solanum tuberosum*), StMYB44 represses anthocyanin accumulation in tubers by directly suppressing the activity of the dihydroflavonol reductase (DFR) promoter [69]. In the current study, RNA-seq and RT-qPCR showed that *DaMYB56*, a member of the S4 subfamily of R2R3-MYB transcription factors in *D. alata*, was highly expressed in tissues with low anthocyanin accumulation. DaMYB56 belongs to the AtMYB4-like clade, which comprises members reported to negatively regulate stress responseses and the biosynthesis of anthocyanins or phenylpropanoids [27,70]. Furthermore, heterologously overexpressing of *DaMYB56* in tobacco significantly inhibited anthocyanin accumulation in flowers. We determined that DaMYB56 and DabHLH72 interact via Y2H and BiFC assays. We also detected the direct binding of DaMYB56 to the *DaANS* promoter in Y1H assays. Additionally, co-expressing *DaMYB75*,

Fig. 6. DaMYB56 regulates transcription from the *DaANS* promoter by interfering with the activation capacity of the DaMYB75-DabHLH72 complex. (A) Total anthocyanin contents in different tissues of the pp *D. alata* cultivar. (B) Relative *DaMYB56* expression levels in the pp *D. alata* cultivar. (C) Representative photograph of flowers from the wild-type (WT) and *DaMYB56* overexpression transgenic lines (OE-1 and OE-5) in the tobacco cultivar K326 background. Transgene expression was determined by RT-qPCR. (D) Total anthocyanin contents of the WT and *DaMYB56*-OE tobacco lines. (E) Y2H assay testing the interaction of DaMYB56 with DabHLH72. pGBKT7-53 + pGADT7-T was used as a positive control, and pGBKT7-lam + pGADT7-T was used as a negative control. –T–L, SD medium lacking Trp and Leu; –T–L–H–A: SD medium lacking Trp, Leu, His, and Ade. 3-AT and X-α-gal were added as an inhibitor and chromogenic substrate, respectively. (F) BiFC assay in *N. benthamiana* leaves. The full-length *DaMYB56* coding sequence was cloned into the pSPYNE vector, and the full-length *DabHLH72* coding sequence was cloned into the pSPYCE vector. pSPYNE-*AtSPT* + pSPYCE-*AtIND* was used as a positive control. Scale bars, 20 μm. (G) Representative photograph of a *D. alata* leaf from the pw cultivar co-infiltrated with *35S:DaMYB75*, *35S:DabHLH72*, and/or *35S:DaMYB56*. FW, fresh weight. (H, I) Total anthocyanin contents (H) and relative *DaANS* expression levels (I) in the *D. alata* leaves shown in (G). Values are means ± standard error from three biological replicates. Significant differences between the experimental and control groups were determined by Student's *t*-test (**, $P < 0.01$). (J) Y1H assay showing the binding of DaMYB56 to the *DaANS* promoter. SD/–Leu: SD medium lacking Leu. AbA was added as an inhibitor. (K) Dual-luciferase reporter assay in *N. benthamiana* leaves. The reporter construct *proDaANS(S2):LUC* was co-infiltrated with the effector constructs *35S:DaMYB75*, *35S:DabHLH72*, and/or *35S:DaMYB56*. Values are means ± standard error from three biological replicates. Different lowercase letters indicate significant differences, as determined by one-way ANOVA, with $P < 0.05$.

DabHLH72, and *DaMYB56* completely abolished the pigmentation resulting from the co-expression of *DaMYB75* and *DabHLH72*. A dual-luciferase reporter assay indicated that DaMYB56 represses *DaANS* promoter activity. These results suggest that DaMYB56 acts as a negative regulator of anthocyanin biosynthesis by binding to the *DaANS* promoter, where it might interact with DabHLH72 to inhibit this process in *D. alata*.

4.3. DNA methylation modulates DaMYB75-mediated regulation of anthocyanin accumulation in D. alata

DNA methylation is a common mechanism that regulates secondary metabolism in plants by controlling gene expression [71]. Transcription is often inhibited when the promoter region of a gene is methylated [72]. In green-skinned pears (*Pyrus communis*), methylation of the *PcMYB10* promoter resulted in lower *PcMYB10* expression. Consequently, *PcUFGT*, a structural gene critical for anthocyanin biosynthesis that is regulated by PcMYB10, was also downregulated in these plants [73]. The accumulation of anthocyanins in the skin of apple fruits is inversely associated with the DNA methylation levels of the *MdMYB10* promoter region [36,37,74]. In this study, the methylation levels along the *DaMYB75* promoter regions were considerably higher in the tubers of the pw cultivar compared to the pp cultivar in the regions −1214 bp to −988 bp and from −1561 bp to −1300 bp, hinting at a negative correlation between the level of DNA methylation at the *DaMYB75* promoter and anthocyanin biosynthesis.

Therefore, we propose the following molecular mechanism for the regulation of anthocyanin accumulation in *D. alata* tubers. DaMYB75 acts as a key activator of anthocyanin biosynthesis, specifically activating the transcription of the *DaANS* promoter to promote this process. *DaMYB75* is highly expressed when its promoter has a low level of DNA methylation, as observed in the pp cultivar with pure purple tubers, and the degree of activation imparted by DaMYB75 is further enhanced when it interacts with DabHLH72. By contrast, in the pw *D. alata* cultivar with pure white tubers, *DaMYB75* expression is repressed due to the high methylation levels of its promoter. Under these conditions, DaMYB56 acts as a negative regulator, binding to the *DaANS* promoter to inhibit anthocyanin biosynthesis, with the degree of inhibition increasing when it interacts with DabHLH72. It is likely that DaMYB75 and DaMYB56 simultaneously regulate anthocyanin biosynthesis in the fp *D. alata* cultivar with faint purple tubers (Fig. 7). In addition, promoter DNA methylation frequently occurs due to the dissemination of methylation marks originating from adjacent transposons and other repeats. In red-fleshed radish, the *CACTA* transposon-induced DNA methylation of the *RsMYB1* promoter was linked to the white-fleshed phenotype [35]. These findings could shed light on the regulatory mechanisms of anthocyanin accumulation and biosynthesis, laying the foundation for genetically enhancing anthocyanin levels in *D. alata*.

The ellipses with a dashed outline indicate gene silencing. The yellow circles indicate DNA methylation marks.

5. Conclusions

Anthocyanin biosynthesis occurs during the early development of *D. alata* tubers, with cyanidin glycoside representing the predominant anthocyanin present in the purple tubers of *D. alata*. *DaANS* and *DaMYB75* were highly expressed in the tubers of the purple cultivar but much more weakly expressed in the pure white cultivar, which showed high methylation levels over the *DaMYB75* promoter. *DaMYB56* expression followed the opposite pattern and was more highly expressed in the tubers of the pure white cultivar. Our findings suggest that DaMYB75 transcriptionally promotes anthocyanin biosynthesis by specifically activating transcription from the *DaANS* promoter. This activation is enhanced through its interaction with DabHLH72. Although DaMYB56 also binds to the *DaANS* promoter, it acts as a negative regulator and also interacts with DabHLH72 to restrict anthocyanin biosynthesis. This study lays the foundation for understanding the molecular mechanisms behind anthocyanin biosynthesis in *D. alata* and paves the way for breeding new *D. alata* varieties with enhanced anthocyanin contents.

CRediT authorship contribution statement

Xin Chen: Writing – review & editing, Writing – original draft, Validation, Data curation. **Jingyu Sun:** Writing – review & editing, Writing – original draft, Validation, Data curation. **Nan Shan:** Writing – review & editing, Funding acquisition. **Asjad Ali:** Writing – review & editing. **Sha Luo:** Visualization, Formal analysis. **Shenglin Wang:** Visualization, Formal analysis. **Qianglong Zhu:** Validation, Investigation. **Yao Xiao:** Validation, Investigation. **Zihao Li:** Validation, Investigation. **Yufan Fang:** Validation. **Jiali Lin:** Validation. **Xiaorong Chen:** Writing – review & editing, Supervision, Conceptualization. **Qinghong Zhou:** Writing – review & editing, Funding acquisition, Conceptualization. **Yingjin Huang:** Writing – review & editing, Supervision, Project administration, Conceptualization.

Declaration of competing interest

The authors declare that they have no known competing financial interests or personal relationships that could have appeared to influence the work reported in this paper.

Acknowledgments

This research was supported by the National Natural Science Foundation of China (32460767), Jiangxi Provincial Key Research and Development Program (20232BBF60007), and Jiangxi Provincial Natural Science Foundation (20224BAB205024).

Appendix A. Supplementary data

Supplementary data for this article can be found online at https://doi.org/10.1016/j.cj.2025.03.009.

References

[1] C. Moriya, T. Hosoya, S. Agawa, Y. Sugiyama, I. Kozone, K. Shin-Ya, N. Terahara, S. Kumazawa, New acylated anthocyanins from purple yam and their antioxidant activity, Biosci. Biotechnol. Biochem. 79 (2015) 1484–1492.
[2] A. Adomėnienė, P.R. Venskutonis, *Dioscorea* spp.: comprehensive review of antioxidant properties and their relation to phytochemicals and health benefits, Molecules 27 (2022) 2530.
[3] B. Winkel-Shirley, Flavonoid biosynthesis. A colorful model for genetics, biochemistry, cell biology, and biotechnology, Plant Physiol. 126 (2001) 485–493.
[4] A.H. Naing, C.K. Kim, Abiotic stress-induced anthocyanins in plants: their role in tolerance to abiotic stresses, Physiol. Plant. 172 (2021) 1711–1723.
[5] Y. Tanaka, N. Sasaki, A. Ohmiya, Biosynthesis of plant pigments: anthocyanins, betalains and carotenoids, Plant J. 54 (2008) 733–749.
[6] U. Szymanowska, U. Zlotek, M. Karas, B. Baraniak, Anti-inflammatory and antioxidative activity of anthocyanins from purple basil leaves induced by selected abiotic elicitors, Food Chem. 172 (2015) 71–77.
[7] F. Cappellini, A. Marinelli, M. Toccaceli, C. Tonelli, K. Petroni, Anthocyanins: from mechanisms of regulation in plants to health benefits in foods, Front. Plant Sci. 12 (2021) 748049.
[8] T.C. Wallace, Anthocyanins in cardiovascular disease, Adv. Nutr. 2 (2011) 1–7.
[9] L. Valenti, P. Riso, A. Mazzocchi, M. Porrini, S. Fargion, C. Agostoni, Dietary anthocyanins as nutritional therapy for nonalcoholic fatty liver disease, Oxid. Med. Cell. Longev. 2013 (2013) 1–8.
[10] W. Kalt, A. Cassidy, L.R. Howard, R. Krikorian, A.J. Stull, F. Tremblay, R. Zamora-Ros, Recent research on the health benefits of blueberries and their anthocyanins, Adv. Nutr. 11 (2020) 224–236.

[11] H. Ayvaz, T. Cabaroglu, A. Akyildiz, C.U. Pala, R. Temizkan, E. Ağçam, Z. Ayvaz, A. Durazzo, M. Lucarini, R. Direito, Z. Diaconeasa, Anthocyanins: metabolic digestion, bioavailability, therapeutic effects, current pharmaceutical/industrial use, and innovation potential, Antioxidants 12 (2022) 48.
[12] Y. Zhang, E. Butelli, C. Martin, Engineering anthocyanin biosynthesis in plants, Curr. Opin. Plant Biol. 19 (2014) 81–90.
[13] Z. Shen, W. Li, Y. Li, M. Liu, H. Cao, N. Provart, X. Ding, M. Sun, Z. Tang, C. Yue, Y. Cao, D. Yuan, L. Zhang, The red flower wintersweet genome provides insights into the evolution of magnoliids and the molecular mechanism for tepal color development, Plant J. 108 (2021) 1662–1678.
[14] D. Cui, S. Zhao, H. Xu, A.C. Allan, X. Zhang, L. Fan, L. Chen, J. Su, Q. Shu, K. Li, The interaction of MYB, bHLH and WD40 transcription factors in red pear (*Pyrus pyrifolia*) peel, Plant Mol. Biol. 106 (2021) 407–417.
[15] S. Wang, Z. Zhang, L.X. Li, H.B. Wang, H. Zhou, X.S. Chen, S.Q. Feng, Apple MdMYB306-like inhibits anthocyanin synthesis by directly interacting with MdMYB17 and MdbHLH33, Plant J. 110 (2022) 1021–1034.
[16] Z.Z. Wei, K.D. Hu, D.L. Zhao, J. Tang, Z.Q. Huang, P. Jin, Y.H. Li, Z. Han, L.Y. Hu, G. F. Yao, H. Zhang, MYB44 competitively inhibits the formation of the MYB340-bHLH2-NAC56 complex to regulate anthocyanin biosynthesis in purple-fleshed sweet potato, BMC Plant Biol. 20 (2020) 258.
[17] C. Dubos, R. Stracke, E. Grotewold, B. Weisshaar, C. Martin, L. Lepiniec, MYB transcription factors in *Arabidopsis*, Trends Plant Sci. 15 (2010) 573–581.
[18] A. Feller, K. Machemer, E.L. Braun, E. Grotewold, Evolutionary and comparative analysis of MYB and bHLH plant transcription factors, Plant J. 66 (2011) 94–116.
[19] X. Li, L. Cao, B. Jiao, H. Yang, C. Ma, Y. Liang, The bHLH transcription factor AcB2 regulates anthocyanin biosynthesis in onion (*Allium cepa* L.), Hortic. Res. 9 (2022) uhac128.
[20] N.W. Albert, D.H. Lewis, H. Zhang, K.E. Schwinn, P.E. Jameson, K.M. Davies, Members of an R2R3-MYB transcription factor family in Petunia are developmentally and environmentally regulated to control complex floral and vegetative pigmentation patterning, Plant J. 65 (2011) 771–784.
[21] S. Vimolmangkang, Y. Han, G. Wei, S.S. Korban, An apple MYB transcription factor, MdMYB3, is involved in regulation of anthocyanin biosynthesis and flower development, BMC Plant Biol. 13 (2013) 176.
[22] H. Liu, Z. Liu, Y. Wu, L. Zheng, G. Zhang, Regulatory mechanisms of anthocyanin biosynthesis in apple and pear, Int. J. Mol. Sci. 22 (2021) 8441.
[23] X.H. An, Y. Tian, K.Q. Chen, X.J. Liu, D.D. Liu, X.B. Xie, C.G. Cheng, P.H. Cong, Y.J. Hao, MdMYB9 and MdMYB11 are involved in the regulation of the JA-induced biosynthesis of anthocyanin and proanthocyanidin in apples, Plant Cell Physiol. 56 (2015) 650–662.
[24] Z.S. Xu, Q.Q. Yang, K. Feng, X. Yu, A.S. Xiong, DcMYB113, a root-specific R2R3-MYB, conditions anthocyanin biosynthesis and modification in carrot, Plant Biotechnol. J. 18 (2020) 1585–1597.
[25] G. Meng, S.K. Clausen, S.K. Rasmussen, Transcriptome analysis reveals candidate genes related to anthocyanin biosynthesis in different carrot genotypes and tissues, Plants 9 (2020) 344.
[26] D. Ma, C.P. Constabel, MYB repressors as regulators of phenylpropanoid metabolism in plants, Trends Plant Sci. 24 (2019) 275–289.
[27] X.C. Wang, J. Wu, M.L. Guan, C.H. Zhao, P. Geng, Q. Zhao, *Arabidopsis* MYB4 plays dual roles in flavonoid biosynthesis, Plant J. 101 (2020) 637–652.
[28] D. Kim, S.J. Jeon, S. Yanders, S.C. Park, H.S. Kim, S. Kim, MYB3 plays an important role in lignin and anthocyanin biosynthesis under salt stress condition in *Arabidopsis*, Plant Cell Rep. 41 (2022) 1549–1560.
[29] X. Li, M. Zhong, L. Qu, J. Yang, X. Liu, Q. Zhao, X. Liu, X. Zhao, AtMYB32 regulates the ABA response by targeting *ABI3*, *ABI4* and *ABI5* and the drought response by targeting *CBF4* in *Arabidopsis*, Plant Sci. 310 (2021) 110983.
[30] H. Zhou, K. Lin-Wang, F. Wang, R.V. Espley, F. Ren, J. Zhao, C. Ogutu, H. He, Q. Jiang, A.C. Allan, Y. Han, Activator-type R2R3-MYB genes induce a repressor-type R2R3-MYB gene to balance anthocyanin and proanthocyanidin accumulation, New Phytol. 221 (2019) 1919–1934.
[31] J.R. Pérez-Díaz, J. Pérez-Díaz, J. Madrid-Espinoza, E. González-Villanueva, Y. Moreno, S. Ruiz-Lara, New member of the R2R3-MYB transcription factors family in grapevine suppresses the anthocyanin accumulation in the flowers of transgenic tobacco, Plant Mol. Biol. 90 (2015) 63–76.
[32] K. Yoshida, D. Ma, C.P. Constabel, The MYB182 protein down-regulates proanthocyanidin and anthocyanin biosynthesis in poplar by repressing both structural and regulatory flavonoid genes, Plant Physiol. 167 (2015) 693–710.
[33] H. Xu, N. Wang, J. Liu, C. Qu, Y. Wang, S. Jiang, N. Lu, D. Wang, Z. Zhang, X. Chen, The molecular mechanism underlying anthocyanin metabolism in apple using the *MdMYB16* and *MdbHLH33* genes, Plant Mol. Biol. 94 (2017) 149–165.
[34] G.M. Deng, S. Zhang, Q.S. Yang, H.J. Gao, O. Sheng, F.C. Bi, C.Y. Li, T. Dong, G.J. Yi, W.D. He, C.H. Hu, MaMYB4, an R2R3-MYB repressor transcription factor, negatively regulates the biosynthesis of anthocyanin in banana, Front. Plant Sci. 11 (2020) 600704.
[35] A. Vicente, L. Zhang, L. Sun, H. Sun, Y. Wang, Q. Wang, Transposon-induced methylation of the *RsMYB1* promoter disturbs anthocyanin accumulation in red-fleshed radish, J. Exp. Bot. 71 (2020) 2537–2550.
[36] J. Zhu, Y. Wang, Q. Wang, B. Li, X. Wang, X. Zhou, H. Zhang, W. Xu, S. Li, L. Wang, The combination of DNA methylation and positive regulation of anthocyanin biosynthesis by MYB and bHLH transcription factors contributes to the petal blotch formation in Xibei tree peony, Hortic. Res. 10 (2023) uhad100.
[37] Y. Liu, X.H. Gao, L. Tong, M.Z. Liu, X.K. Zhou, M.M. Tahir, L.B. Xing, J.J. Ma, N. An, C.P. Zhao, J.L. Yao, D. Zhang, Multi-omics analyses reveal MdMYB10 hypermethylation being responsible for a bud sport of apple fruit color, Hortic. Res. 9 (2022), uhac179.
[38] A. Sicilia, E. Scialò, I. Puglisi, A.R. Lo Piero, Anthocyanin biosynthesis and DNA methylation dynamics in sweet orange fruit [*Citrus sinensis* L. (Osbeck)] under cold stress, J. Agric. Food. Chem. 68 (2020) 7024–7031.
[39] H.N. Liu, Q. Shu, K. Lin-Wang, R.V. Espley, A.C. Allan, M.S. Pei, X.L. Li, J. Su, J. Wu, DNA methylation reprogramming provides insights into light-induced anthocyanin biosynthesis in red pear, Plant Sci. 326 (2023) 111499.
[40] M. Tamiru, S. Yamanaka, C. Mitsuoka, P. Babil, H. Takagi, A. Lopez-Montes, A. Sartie, R. Asiedu, R. Terauchi, Development of genomic simple sequence repeat markers for yam, Crop Sci. 55 (2015) 2191–2200.
[41] X. Chen, J. Sun, Q. Zhu, Y. Xiao, H. Zhang, Y. Huang, P. Wang, T. Cao, R. Hu, Z. Xiang, N. Shan, Q. Zhou, Characterizing diversity based on phenotypes and molecular marker analyses of purple yam (*Dioscorea alata* L.) germplasm in southern China, Genet. Resour. Crop Evol. 69 (2022) 2501–2513.
[42] Z.G. Wu, W. Jiang, N. Mantri, X.Q. Bao, S.L. Chen, Z.M. Tao, Transciptome analysis reveals flavonoid biosynthesis regulation and simple sequence repeats in yam (*Dioscorea alata* L.) tubers, BMC Genomics 16 (2015) 346.
[43] J.M. Yin, R.X. Yan, P.T. Zhang, X.Y. Han, L. Wang, Anthocyanin accumulation rate and the biosynthesis related gene expression in *Dioscorea alata*, Biol. Plant. 59 (2015) 325–330.
[44] T. Vatai, M. Škerget, Ž. Knez, Extraction of phenolic compounds from elder berry and different grape marc varieties using organic solvents and/or supercritical carbon dioxide, J. Food Eng. 90 (2009) 246–254.
[45] J.V. Bredeson, J.B. Lyons, I.O. Oniyinde, N.R. Okereke, O. Kolade, I. Nnabue, C.O. Nwadili, E. Hřibová, M. Parker, J. Nwogha, S. Shu, J. Carlson, R. Kariba, S. Muthemba, K. Knop, G.J. Barton, A.V. Sherwood, A. Lopez-Montes, R. Asiedu, R. Jamnadass, A. Muchugi, D. Goodstein, C.N. Egesi, J. Featherston, A. Asfaw, G.G. Simpson, J. Doležel, P.S. Hendre, A. Van Deynze, P.L. Kumar, J.E. Obidiegwu, R. Bhattacharjee, D.S. Rokhsar, Chromosome evolution and the genetic basis of agronomically important traits in greater yam, Nat. Commun. 13 (2022) 2001.
[46] S. Kumar, G. Stecher, K. Tamura, MEGA7: molecular evolutionary genetics analysis version 7.0 for bigger datasets, Mol. Biol. Evol. 33 (2016) 1870–1874.
[47] I.A. Sparkes, J. Runions, A. Kearns, C. Hawes, Rapid, transient expression of fluorescent fusion proteins in tobacco plants and generation of stably transformed plants, Nat. Protoc. 1 (2006) 2019–2025.
[48] A.B. Dommes, T. Gross, D.B. Herbert, K.I. Kivivirta, A. Becker, Virus-induced gene silencing: empowering genetics in non-model organisms, J. Exp. Bot. 70 (2019) 757–770.
[49] S. Pattanaik, Q. Kong, D. Zaitlin, J.R. Werkman, C.H. Xie, B. Patra, L. Yuan, Isolation and functional characterization of a floral tissue-specific R2R3 MYB regulator from tobacco, Planta 231 (2010) 1061–1076.
[50] C. Zhong, Y. Tang, B. Pang, X. Li, Y. Yang, J. Deng, C. Feng, L. Li, G. Ren, Y. Wang, J. Peng, S. Sun, S. Liang, X. Wang, The R2R3-MYB transcription factor GhMYB1a regulates flavonol and anthocyanin accumulation in *Gerbera hybrida*, Hortic. Res. 7 (2020) 78.
[51] Z. Lv, Y. Huang, B. Ma, Z. Xiang, N. He, LysM1 in MmLYK2 is a motif required for the interaction of MmLYP1 and MmLYK2 in the chitin signaling, Plant Cell Rep. 37 (2018) 1101–1112.
[52] Q. Xu, X. Deng, Y. Yuan, J. Fu, Z. Tang, D. Huang, CsMYB3 and CsRuby1 form an 'activator-and-repressor' loop for the regulation of anthocyanin biosynthesis in citrus, Plant Cell Physiol. 61 (2020) 318–330.
[53] R.P. Hellens, A.C. Allan, E.N. Friel, K. Bolitho, K. Grafton, M.D. Templeton, S. Karunairetnam, A.P. Gleave, W.A. Laing, Transient expression vectors for functional genomics, quantification of promoter activity and RNA silencing in plants, Plant Methods 1 (2005) 13.
[54] R.E. Haurwitz, M. Jinek, B. Wiedenheft, K. Zhou, J.A. Doudna, Sequence- and structure-specific RNA processing by a CRISPR endonuclease, Science 329 (2010) 1355–1358.
[55] K. Lin-Wang, K. Bolitho, K. Grafton, A. Kortstee, S. Karunairetnam, T.K. McGhie, R.V. Espley, R.P. Hellens, A.C. Allan, An R2R3 MYB transcription factor associated with regulation of the anthocyanin biosynthetic pathway in Rosaceae, BMC Plant Biol. 10 (2010) 50.
[56] J.A. Rodrigues, R.V. Espley, A.C. Allan, Genomic analysis uncovers functional variation in the C-terminus of anthocyanin-activating MYB transcription factors, Hortic. Res. 8 (2021) 77.
[57] R. Zhao, X. Song, N. Yang, L. Chen, L. Xiang, X.Q. Liu, K. Zhao, Expression of the subgroup IIIf bHLH transcription factor CpbHLH1 from *Chimonanthus praecox* (L.) in transgenic model plants inhibits anthocyanin accumulation, Plant Cell Rep. 39 (2020) 891–907.
[58] Y. Fan, J. Peng, J. Wu, P. Zhou, R. He, A.C. Allan, L. Zeng, NtbHLH1, a JAF13-like bHLH, interacts with NtMYB6 to enhance proanthocyanidin accumulation in Chinese Narcissus, BMC Plant Biol. 21 (2021) 275.
[59] Y. Li, X. Shan, R. Gao, S. Yang, S. Wang, X. Gao, L. Wang, Two IIIf clade-bHLHs from *Freesia hybrida* play divergent roles in flavonoid biosynthesis and trichome formation when ectopically expressed in *Arabidopsis*, Sci. Rep. 6 (2016) 30514.
[60] A.H. Naing, C.K. Kim, Roles of R2R3-MYB transcription factors in transcriptional regulation of anthocyanin biosynthesis in horticultural plants, Plant Mol. Biol. 98 (2018) 1–18.
[61] Y.W. Zhao, C.K. Wang, X.Y. Huang, D.G. Hu, Anthocyanin stability and degradation in plants, Plant Signal. Behav. 16 (2021) 1987767.
[62] V.R. Vishnu, A.N. Jyothi, M.N. Sheela, J. Sreekumar, Identification of anthocyanins in a purple yam (*Dioscorea alata*) accession and their in vitro antiproliferative activity, J. Plant Biochem. Biotechnol. 32 (2023) 467–477.

[63] Z. Fang, D. Wu, D. Yü, X. Ye, D. Liu, J. Chen, Phenolic compounds in Chinese purple yam and changes during vacuum frying, Food Chem. 128 (2011) 943–948.
[64] Y. Zhao, W. Dong, Y. Zhu, A.C. Allan, K. Lin-Wang, C. Xu, *PpGST1*, an anthocyanin-related glutathione S-transferase gene, is essential for fruit coloration in peach, Plant Biotechnol. J. 18 (2020) 1284–1295.
[65] H. Li, Z. Yang, Q. Zeng, S. Wang, Y. Luo, Y. Huang, Y. Xin, N. He, Abnormal expression of *bHLH3* disrupts a flavonoid homeostasis network, causing differences in pigment composition among mulberry fruits, Hortic. Res. 7 (2020) 83.
[66] C. Deng, J. Wang, C. Lu, Y. Li, D. Kong, Y. Hong, H. Huang, S. Dai, CcMYB6-1 and CcbHLH1, two novel transcription factors synergistically involved in regulating anthocyanin biosynthesis in cornflower, Plant Physiol. Biochem. 151 (2020) 271–283.
[67] N. Jia, J.J. Wang, J. Liu, J. Jiang, J. Sun, P. Yan, Y. Sun, P. Wan, W. Ye, B. Fan, DcTT8, a bHLH transcription factor, regulates anthocyanin biosynthesis in *Dendrobium candidum*, Plant Physiol. Biochem. 162 (2021) 603–612.
[68] H. Yan, X. Pei, H. Zhang, X. Li, X. Zhang, M. Zhao, V.L. Chiang, R.R. Sederoff, X. Zhao, MYB-mediated regulation of anthocyanin biosynthesis, Int. J. Mol. Sci. 22 (2021) 3103.
[69] Y. Liu, K. Lin-Wang, R.V. Espley, L. Wang, Y. Li, Z. Liu, P. Zhou, L. Zeng, X. Zhang, J. Zhang, A.C. Allan, StMYB44 negatively regulates anthocyanin biosynthesis at high temperatures in tuber flesh of potato, J. Exp. Bot. 70 (2019) 3809–3824.
[70] W.Y. Bang, S.W. Kim, I.S. Jeong, H. Koiwa, J.D. Bahk, The C-terminal region (640–967) of *Arabidopsis* CPL1 interacts with the abiotic stress- and ABA-responsive transcription factors, Biochem. Biophys. Res. Commun. 372 (2008) 907–912.
[71] Y. Zang, L. Xie, J. Su, Z. Luo, X. Jia, X. Ma, Advances in DNA methylation and demethylation in medicinal plants: a review, Mol. Biol. Rep. 50 (2023) 7783–7796.
[72] H.M. Zhang, Z.B. Lang, J.K. Zhu, Dynamics and function of DNA methylation in plants, Nat. Rev. Mol. Cell Biol. 19 (2018) 489–506.
[73] Z. Wang, D. Meng, A. Wang, T. Li, S. Jiang, P. Cong, T. Li, The methylation of the *PcMYB10* promoter is associated with green-skinned sport in max red bartlett pear, Plant Physiol. 162 (2013) 885–896.
[74] Y.C. Zhu, B. Zhang, A.C. Allan, K. Lin-Wang, Y. Zhao, K. Wang, K.S. Chen, C.J. Xu, DNA demethylation is involved in the regulation of temperature-dependent anthocyanin accumulation in peach, Plant J. 102 (2020) 965–976.